Course on Geotechnical Risk in Tunnels
Aveiro, Portugal 2004

Fault Zones and TBM

Nick Barton, (Nick Barton & Associates)

Abstract

This paper is based on the lecture with this title that was given at the Aveiro Course on Geotechnical Risk in Tunnels in 2004. The present subject matter: *fault zones and TBM*, is richly illustrated with case record figures and pictures, mostly from the personal experiences of the author. The following main topics are covered:

1. Fault zone experiences in TBM tunnels in Italy, Greece, Kashmir, Hong Kong and Taiwan. 2. Fault zone cases in the Qtbm data base. 3. Attempts to be prepared using seismic and core logging and the Qtbm prognosis model.

Introduction

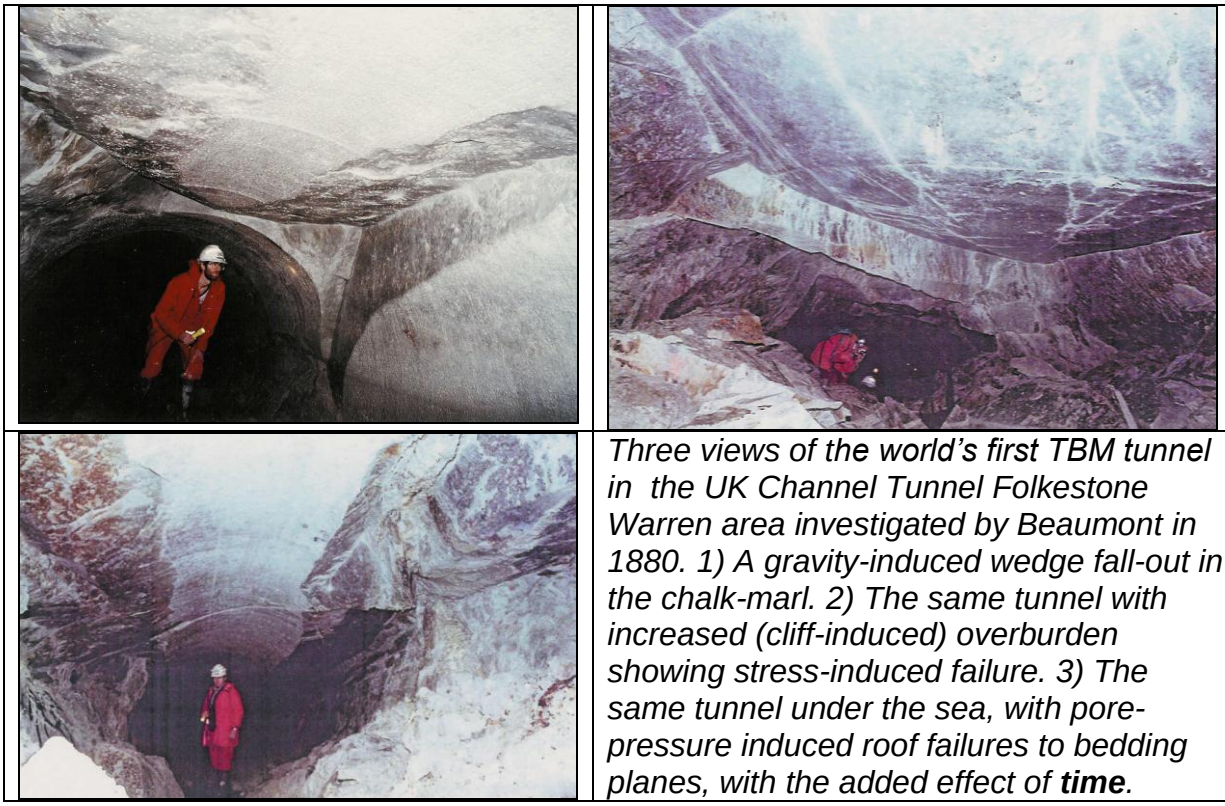

Three views of the world's first TBM tunnel in the UK Channel Tunnel Folkestone Warren area investigated by Beaumont in 1880. 1) A gravity-induced wedge fall-out in the chalk-marl. 2) The same tunnel with increased (cliff-induced) overburden showing stress-induced failure. 3) The same tunnel under the sea, with pore-pressure induced roof failures to bedding planes, with the added effect of ***time****.*

Figure 1. Three types of failure in the world's oldest TBM tunnel (Beaumont, 1880).

The failures shown in Figure 1 show classic rock mechanics features, which in the case of #3 are clearly enhanced by the effect of time. A rockmass classification of this tunnel, in relation to systematic Q-logging of the Channel Tunnel's main running tunnels driven 110 years later, was given by Barton and Warren, 1990.

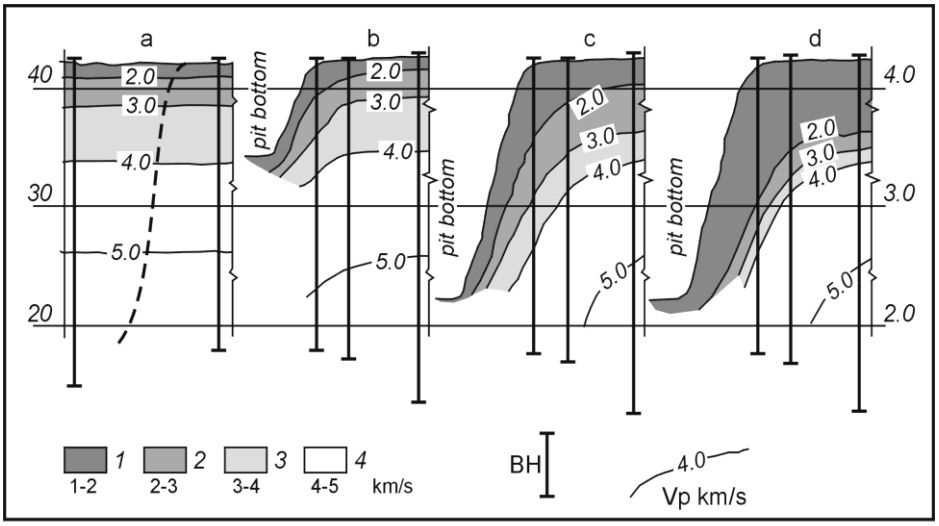

Figure 2. Effect of stress change and time on cross-hole seismic velocity at a Russian ship-lock. There is a 1 year delay between 'c' and 'd'. The reduced velocities are presumably caused by insufficient rock support where shear stresses are high, as also experienced in a 'flat' TBM tunnel face.

The flat face of a large diameter TBM tunnel is not unlike a vertical rock slope. When a TBM cutter-head is withdrawn from a fault zone to (post) treat the rock mass, there may be a loosening effect such as illustrated from the slope excavation shown in Figure 2. The case of loosening in a fault zone shown in Figure 3 is from Grandori et al. 1995, from the Evinos-Mornos Tunnel in Greece.

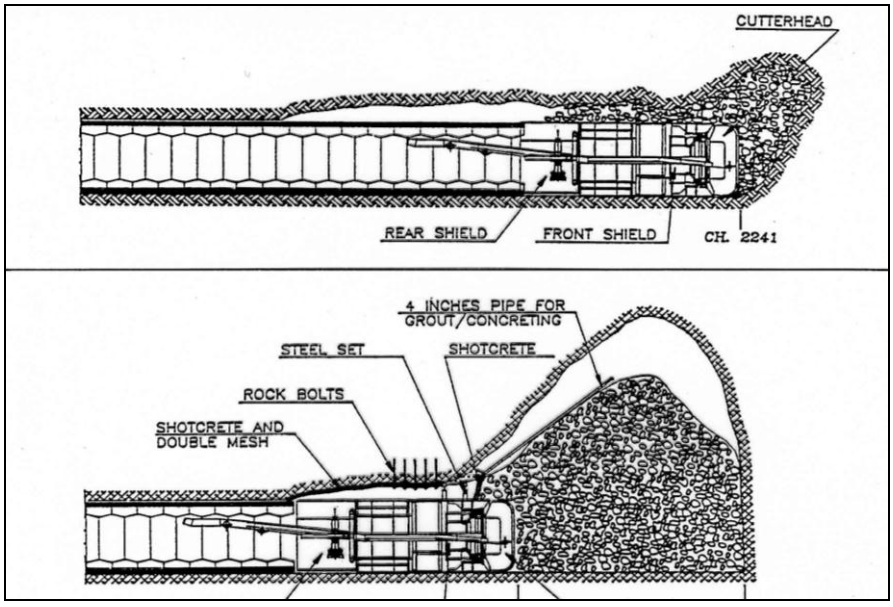

Figure 3. Loosening in a fault zone from Grandori et al. 1995, at the Evinos-Mornos Tunnel in Greece. We will return to this case later.

The case of Pont Ventoux, N. Italy

A fault zone destroys much of the familiar tangential stress arch, and tunnel stability problems often arise as a result. High pressure inflow and falls of clay and rock blocks are other factors. The Italian Pont Ventoux HEP headrace tunnel was increasingly making a tangent to numerous faults, as shown in Figure 4.

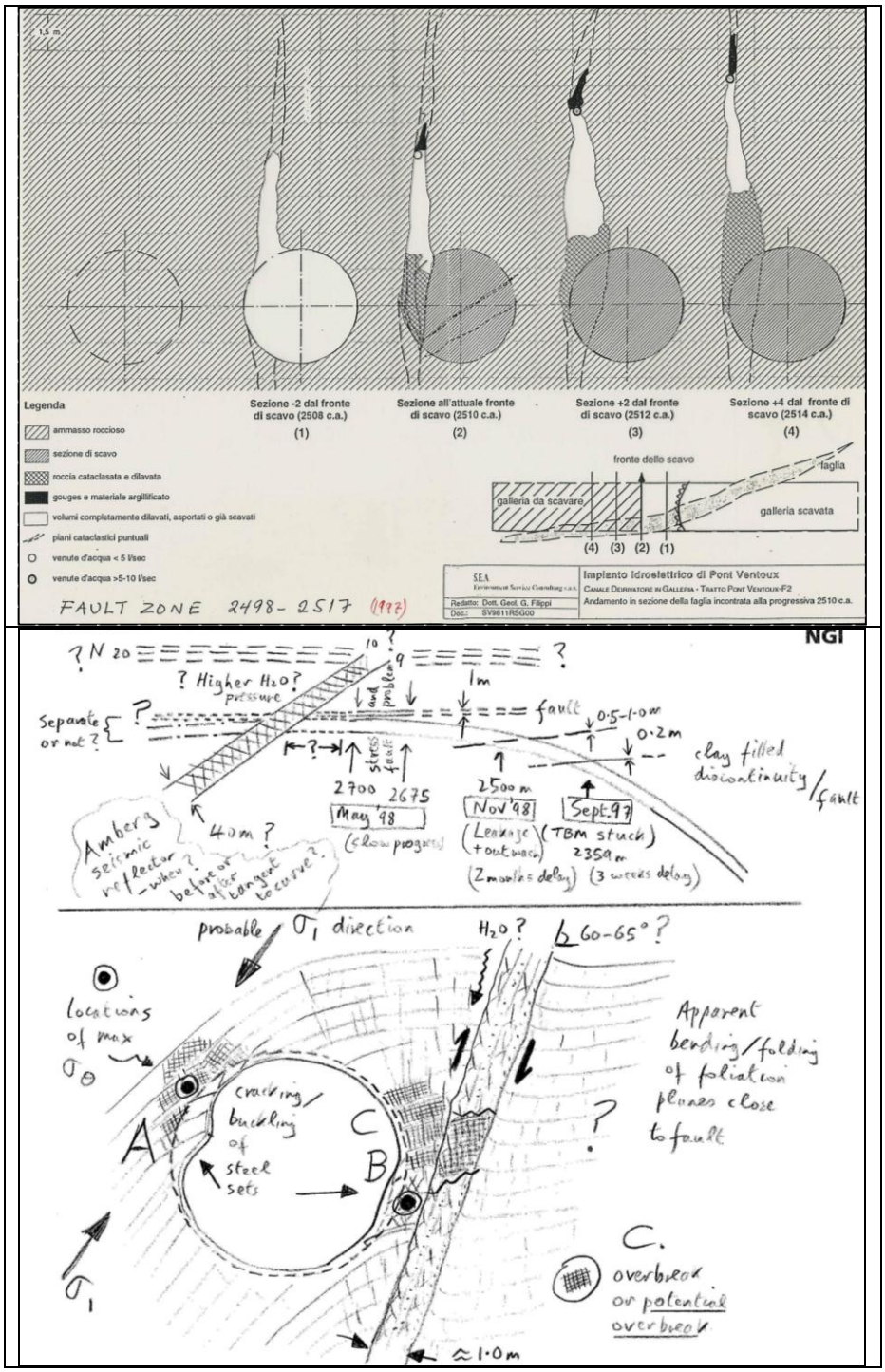

Figure 4. Two of the many fault-zone problems experienced at the Pont Ventoux HEP project in N. Italy. (Barton, 1999; NGI contract report).

The adverse effect on tangential stress (arching) is clear from Figure 4, but adverse water pressures were to prove the biggest problem with respect to the cutter-head getting stuck in these various fault zones at Pont Ventoux.

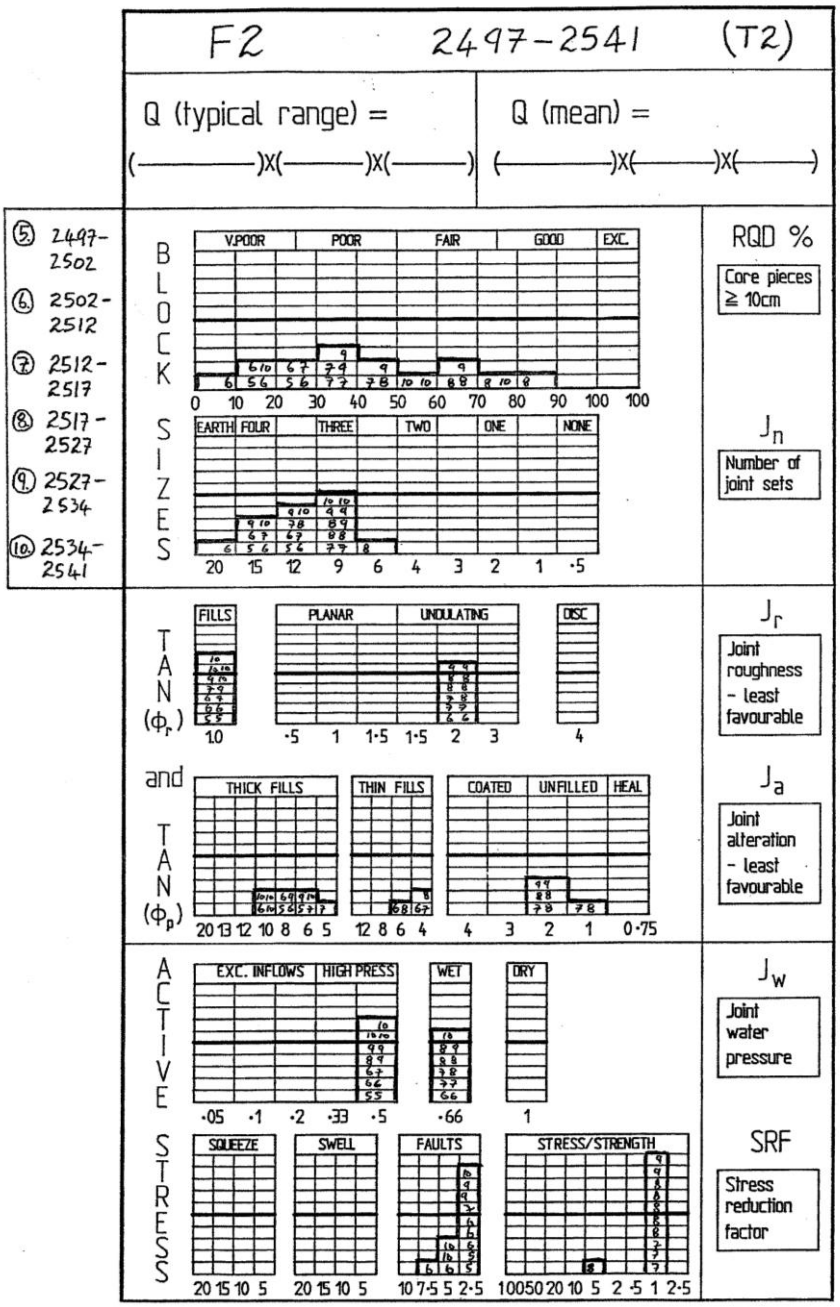

Figure 5. Q-histogram logging of part of an earlier section of the F2 fault at Pont Ventoux, from ch. 2,500m. Mixed RQD, high Jn, low Jr/Ja, low Ja, high SRF, and Q often < 0.1.

Another problem in fault zones is the grippers, and maybe also the shield i.e. delayed treatment of rock that actually requires ***pre-treatment.*** Figure 6, after Wanner, shows the implications in graphic form. Tangential stress indicators have been added in Barton, 2000.

What if the rock is too weak for the gripper action? Grippers usually have ‘rib-spaces’ (e.g. at 0.6m spacing), to avoid crushing steel sets that are placed at this regular spacing. But if too many sets are needed (i.e. sets placed flange-against-flange) due to faulted rock, then there is the likelihood of crushing of the sets just where needed most. Such experiences from Pont Ventoux are shown in Figure 7.

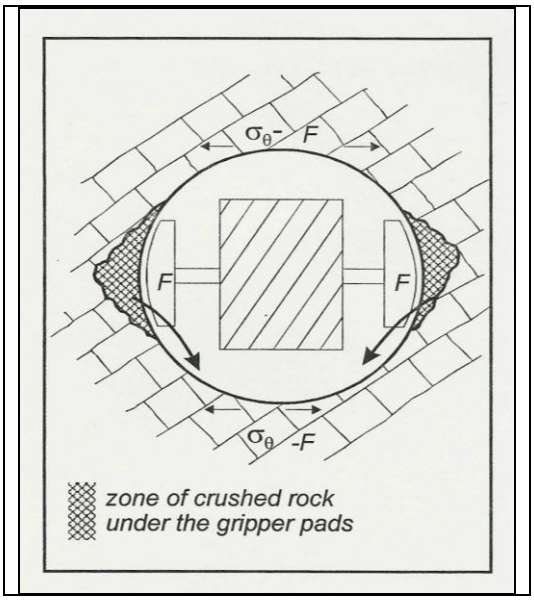

Figure 6. Adverse effect of gripper action where deformability is high, or alternatively; adverse effect of fall-out in haunches on gripper action. After Wanner, 1984, from Barton 2000.

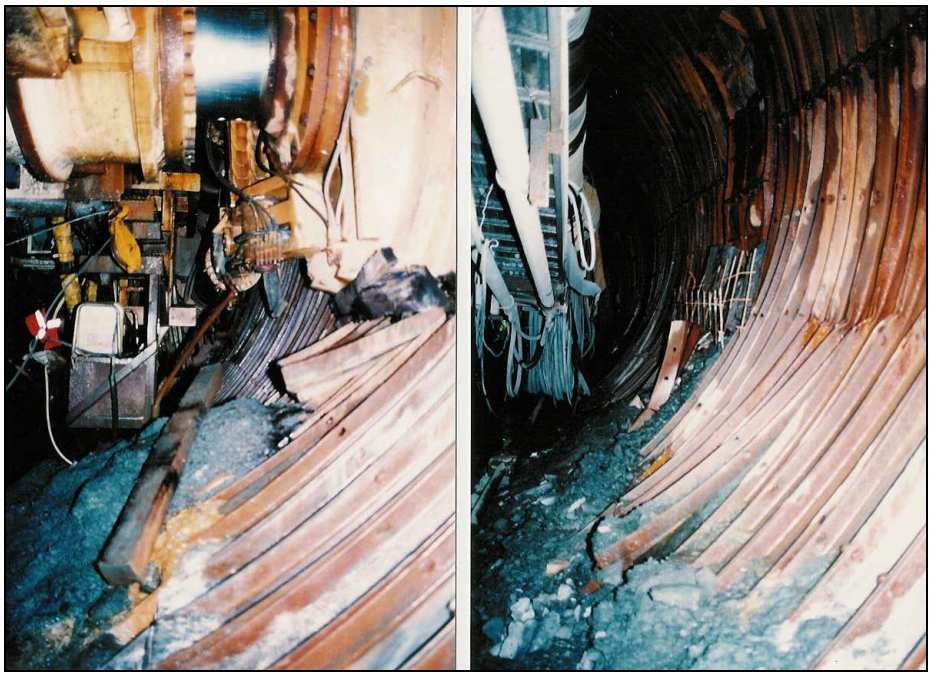

Figure 7. Crushing of flange-to-flange steel sets in fault zone, by gripper action.

Pont Ventoux HEP also had high (non-vertical) σ_1 stress, and very high water inflows, which were very adverse to stability in fault zones full of clay, silt , sand and crushed rock. Figure 8 illustrates this fatal combination where stability was good due to massive rock conditions.

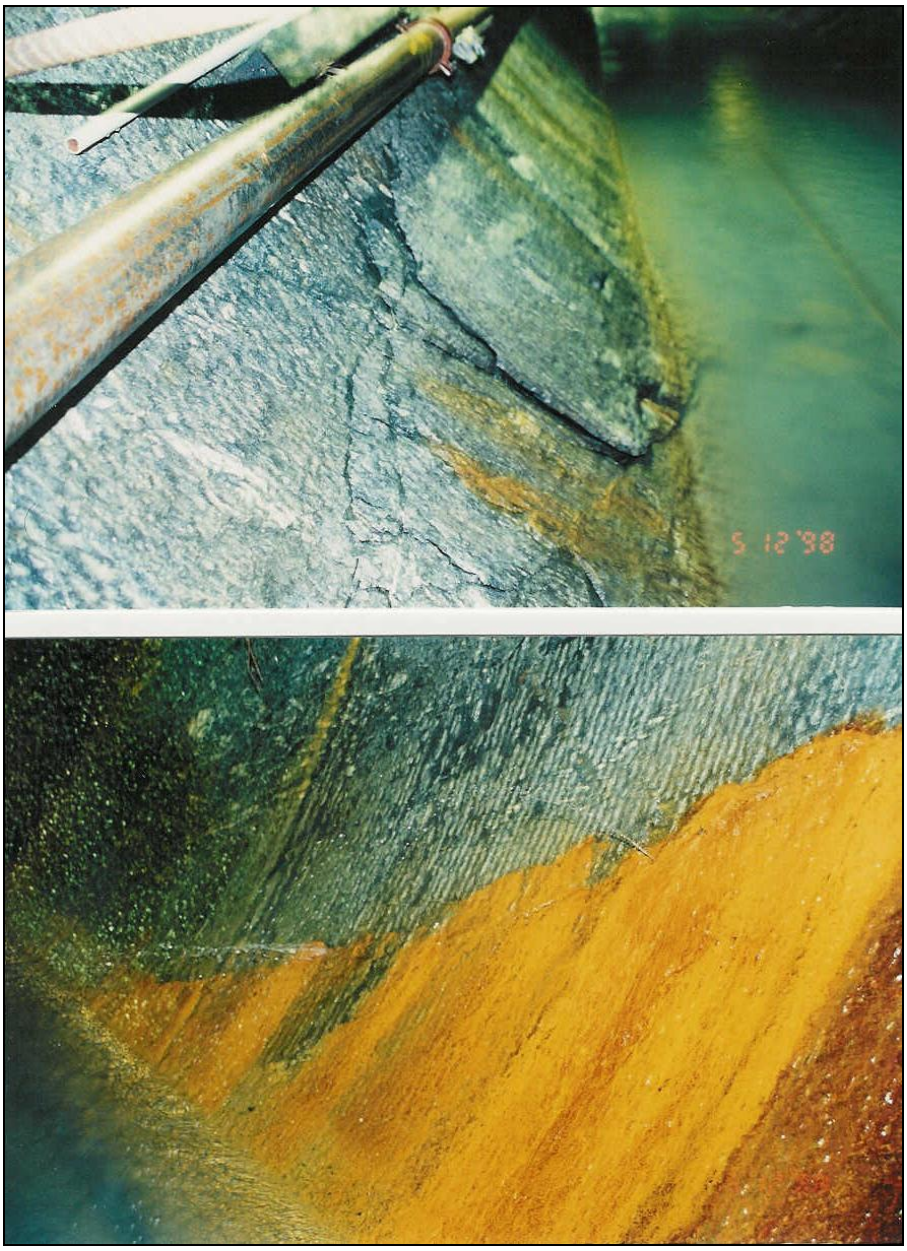

Figure 8. High anisotropic stresses and high water pressures seen where stability was good.

The 7km tunnel was parallel to a marked NW-SE trending valley , and also parallel to the foliation and to the (later discovered) fault zone swarms parallel to the valley side. The structural geology proved to be a disaster for the tunnel route, due to its near-parallel orientation to the later discovered faults.

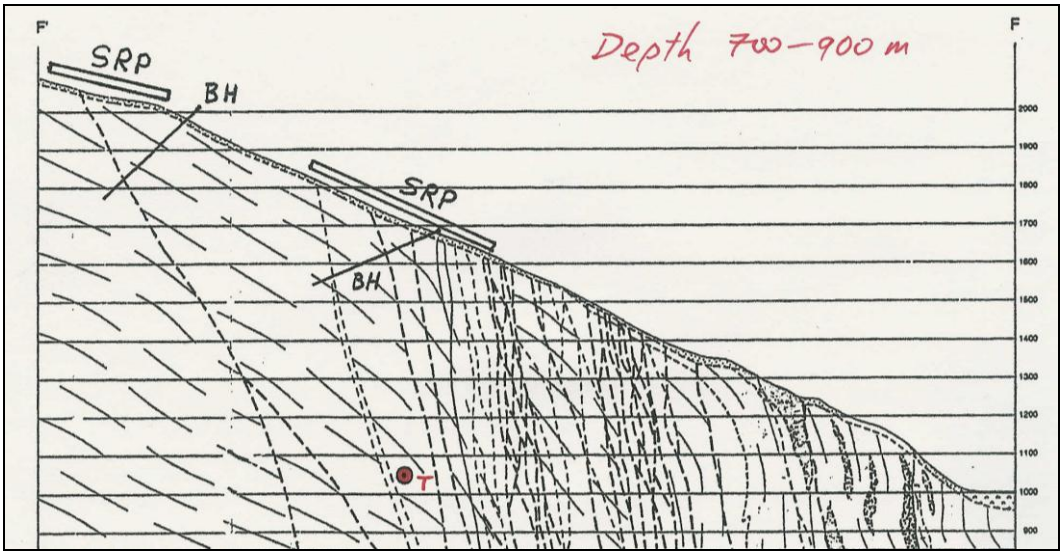

Figure 9. The tunnel was apparently 'too deep' for satisfactory geological investigations, judging by the 'missed' fault swarms shown here. In fact it was clearly not adequately investigated. BH boreholes, and SRP seismic refraction.

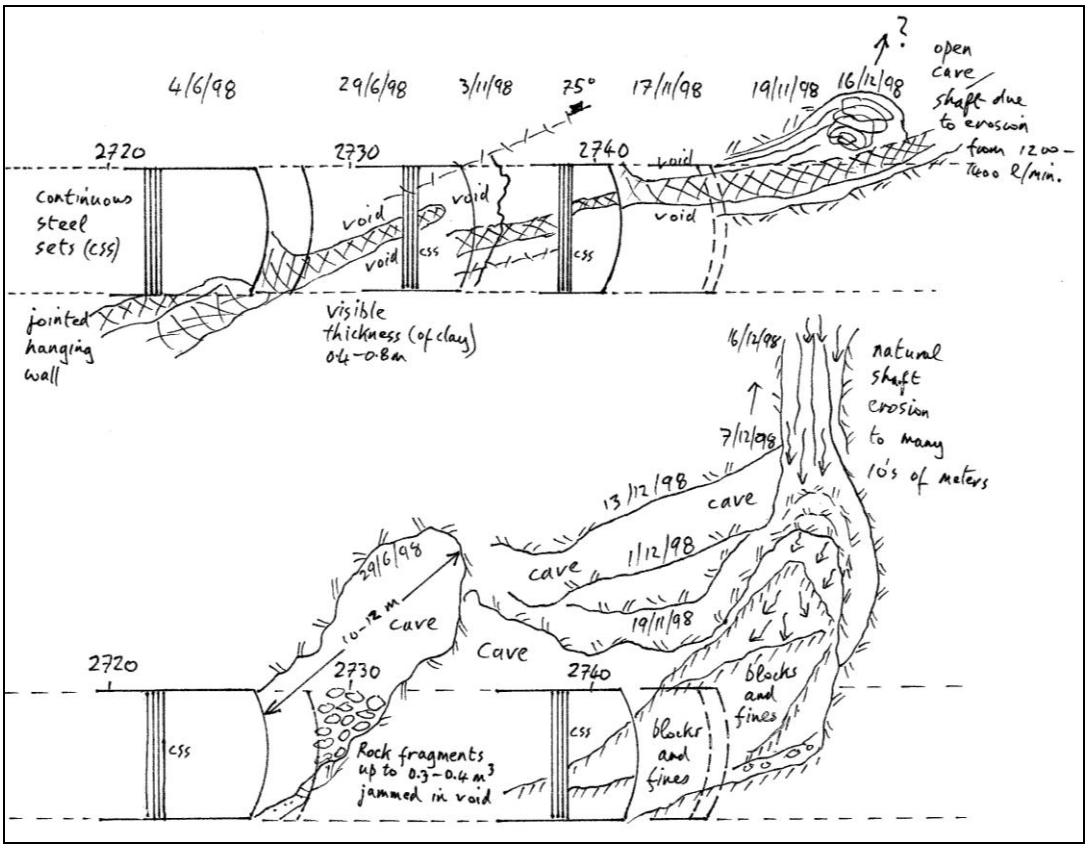

Figure 10. The Pont Ventoux TBM was stuck here for 6 months (due to blocked cutter head) from continuously falling blocks from the 'fault shaft', assisted by water and/or water pressure. These sketches are super-imposed on one sheet, from the geologist's daily logs.

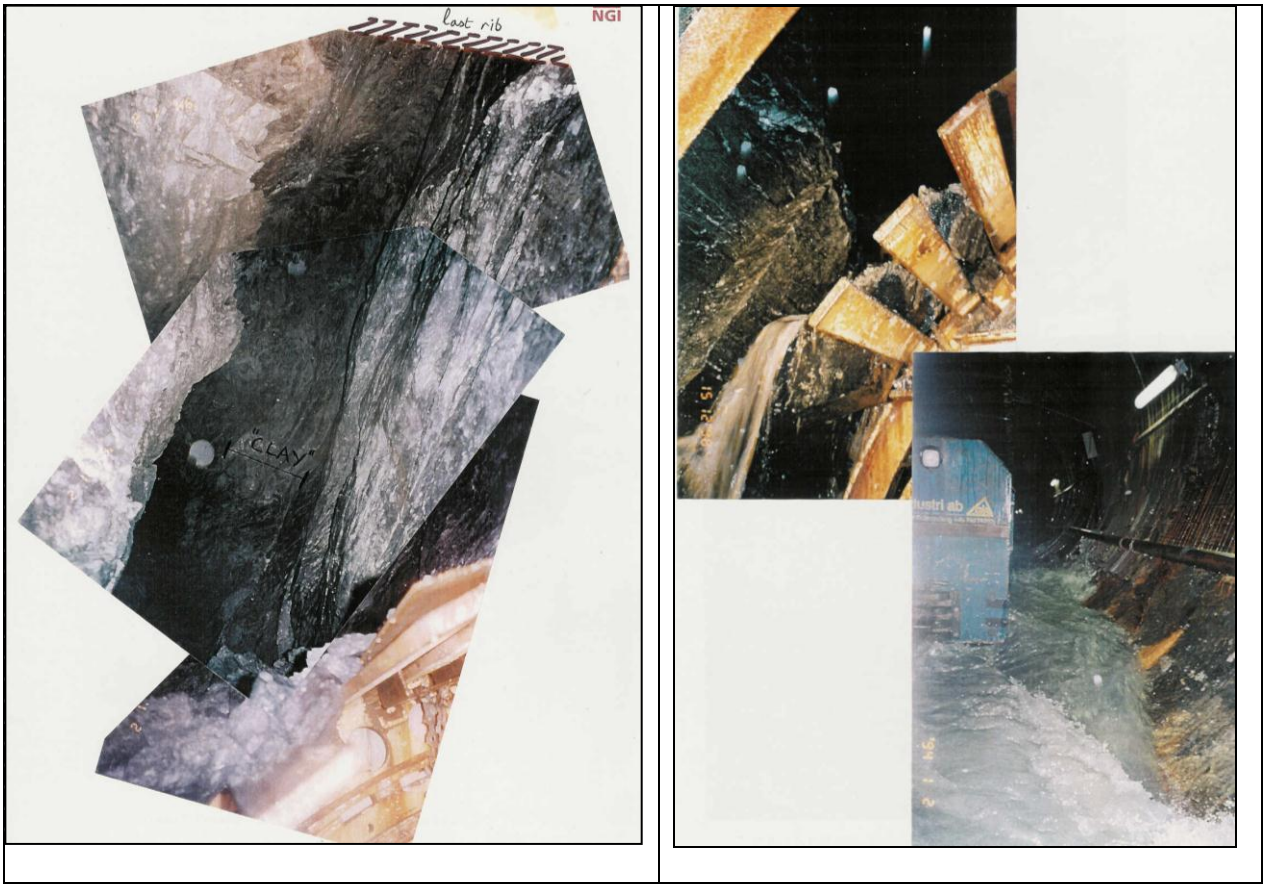

Figure 11. View (120°) into inverted 'fault trench', and view of 'finger shield' and levels of water at the blocked face and behind the back-up.

Derailment of the train was frequent behind the back-up, due to build-up of a 'delta' of sand and silt washed out of the fault zone.

An NGI report written by the author in 1999, contained the following advice.

'Experience has shown that the extremely adverse conditions are caused by a combination of major water inflows, erosion of faulted material, and major void formation due to the generally adverse, sub-parallel fault orientations. The need to build a continuous steel liner (flange-to-flange) and further delays caused by cutter-head jamming, has given only 20m advance in the last 7 months'.

'The outlook for future tunnelling is bleak if further members of the fault swarm lie sub-parallel, close to, or intersect the future tunnel. A drill-and-blast alternative of larger cross-section following the same route, or a revised route for continued TBM boring, or either tunnelling methods along a revised route, are three alternatives that need serious consideration'.

During 2004 the tunnel is expected to be completed by drill-and-blast from the other end of the tunnel, by-passing the rusting and abandoned TBM.

Development of the Q_{TBM} method of prognosis

During the 6 months following the Pont Ventoux experiences, the Q_{TBM} method was developed (Barton, 2000), based on an analysis of 140 TBM case records. The case records showed the following general 'deceleration' trends, when advance rate was plotted for various time periods. The classic equation AR = PR x U (where U= utilization), needs to be modified to the form AR = PR x T^{-m} to accommodate this fact.

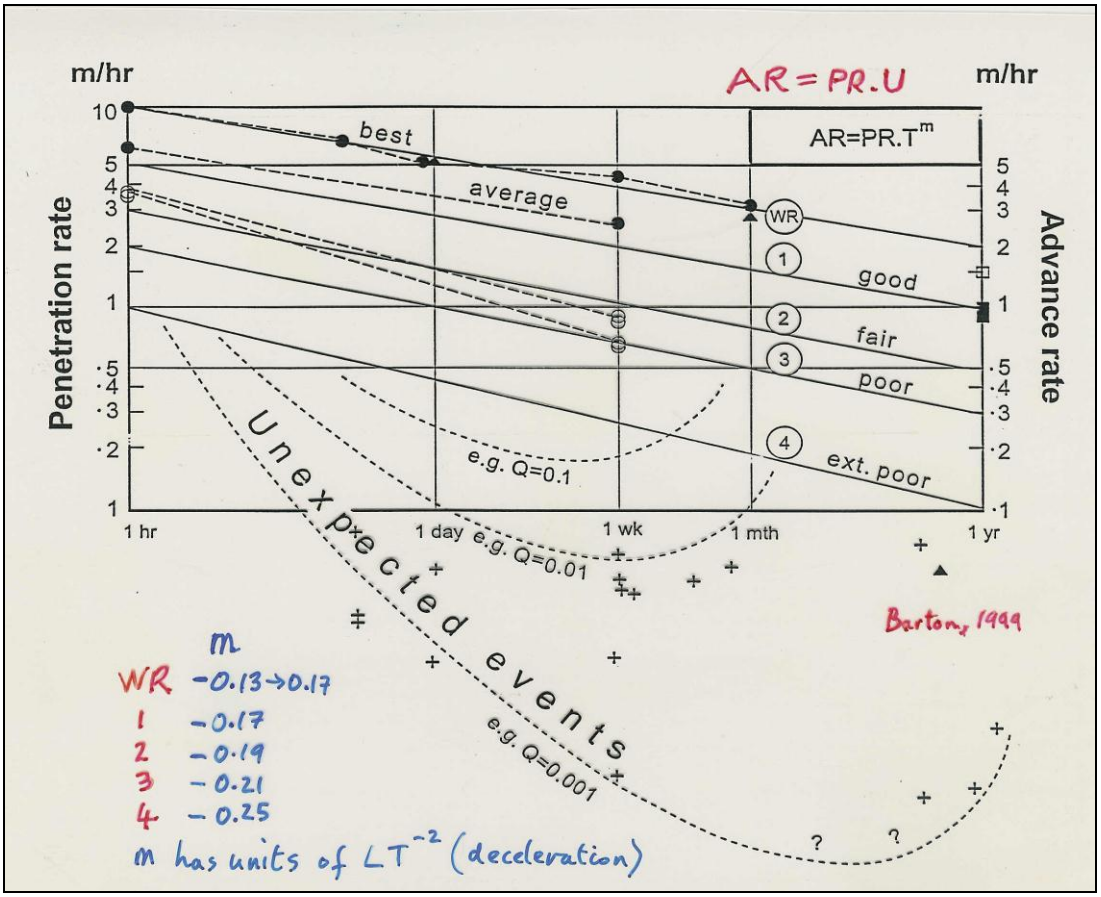

Figure 12. General trends of deceleration, and the adverse effect of 'unexpected events'. (Note PR = penetration rate, AR = actual advance rate, U = utilization = when boring, and T = time in hours). Barton, 1999, 2000.

The previously described Pont Ventoux fault zone performance of 7months for only 20m of advance, represents an average AR = 20/(7x720) = 0.004m/hr. This is almost off the bottom of the above chart, in the 'unpredicted events' area where various case record crosses (+) are plotted.

The gradients of *deceleration* (-m) given by the negative slopes of the TBM performance trend lines in Figure 12 are strongly related to Q-values when the quality is very poor *(i.e. Q < 1.0)* and so-called 'unexpected events' occur.

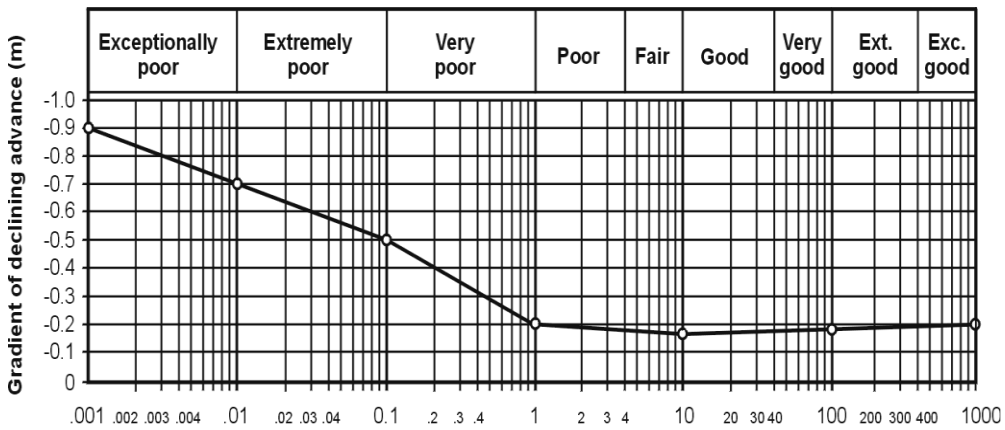

Rock mass quality $Q = \left(\frac{RQD}{J_n}\right) x \left(\frac{J_r}{J_a}\right) x \left(\frac{J_w}{SRF}\right)$

Figure 13. Preliminary estimation of deceleration gradient (-m) from the Q-value, is clearly of relevance for fault zones, as they have Q-values ≤ 0.1

The 140 case records were analysed for 'best', 'average' and 'bad-ground' performance, as shown on the chart of log PR – log AR – log T given in Figure 14. 'Unexpected event' cases are shown as the steepest lines.

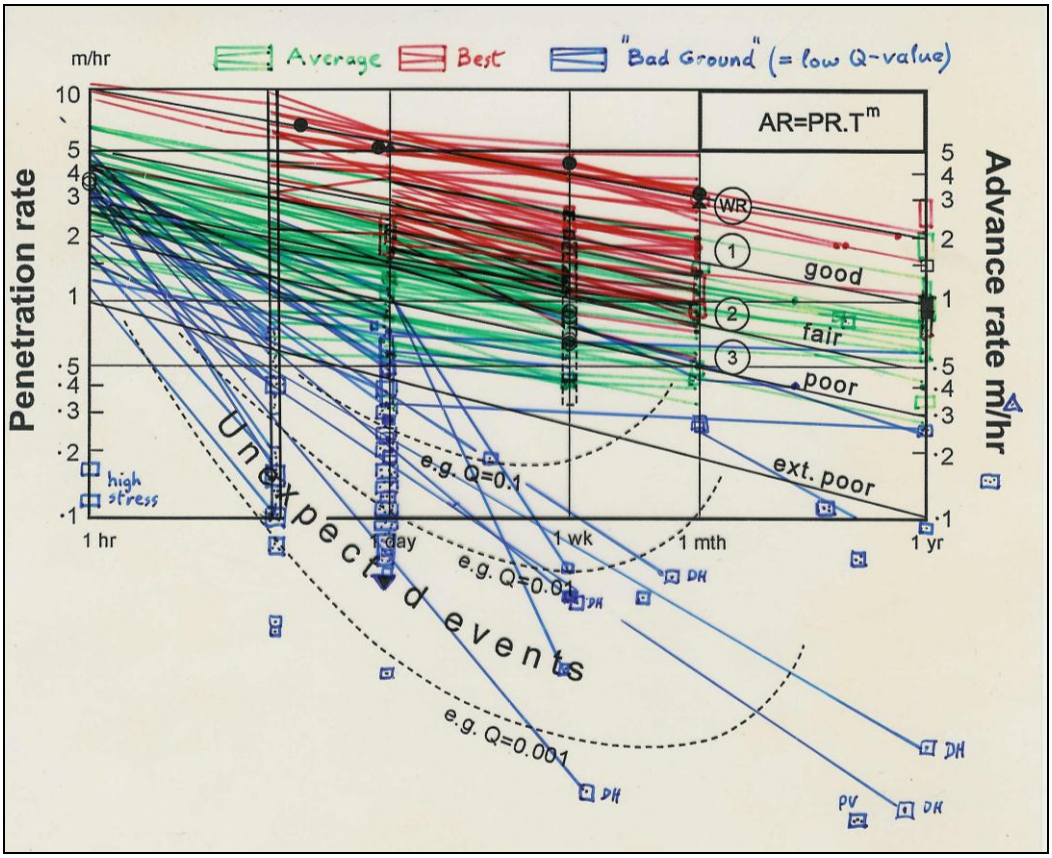

Figure 14. The 140 case records used to develop part of the the Q_{TBM} prognosis model. Barton, 2000.

Using oilwell-stability sketches (from Bradley 1979),we can say that many faults (or boundaries of faults, where there is water), cause a ‘ravelling’ type of behaviour, like #4 in Figure 15.

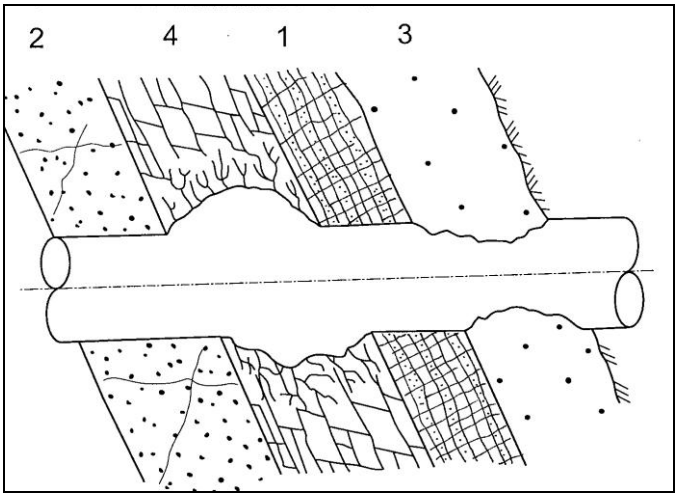

Figure 15. Four characters of ground from oil-well experience (Bradley, 1979)

The clay core of a fault (if present), may suffer squeeze, like #3. The well jointed case (#1) may be ideal for TBM due also to its favourable orientation, assuming little support is needed (giving both high PR *and* high AR). However, the sparsely jointed case (#2) may be tough to bore in hard abrasive rock (low PR, and consequently low AR).

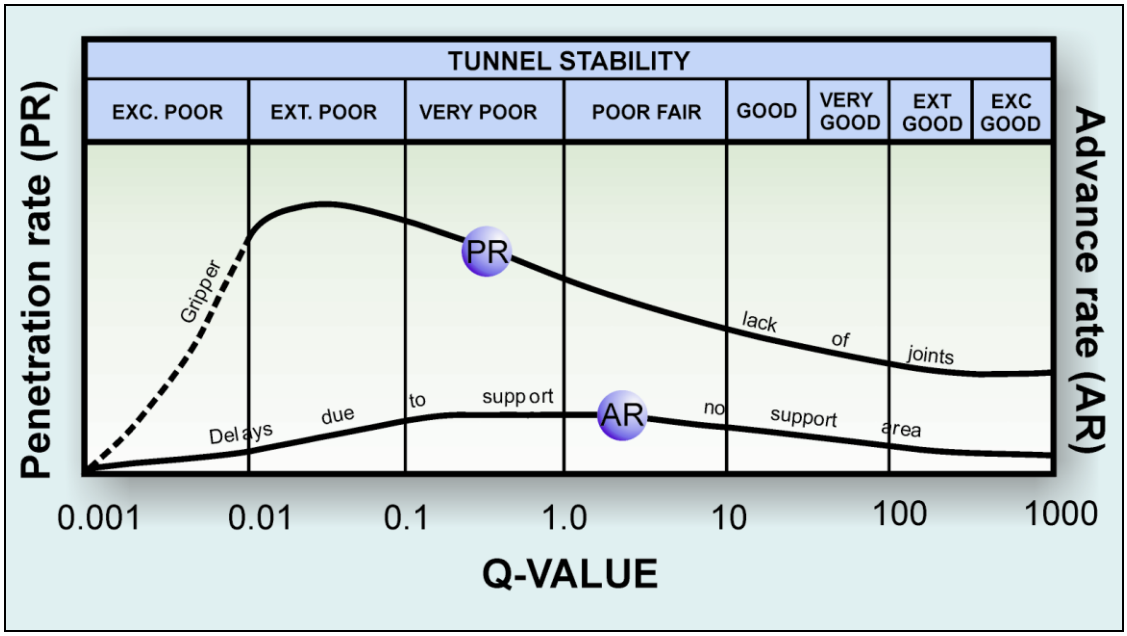

Figure 16. The Q-value descriptions of tunnel stability, which have general applicability, are however not sufficient on their own to describe TBM performance, due to the special ***cutter- rock*** *and TB****M - rockmass*** *interactions.*

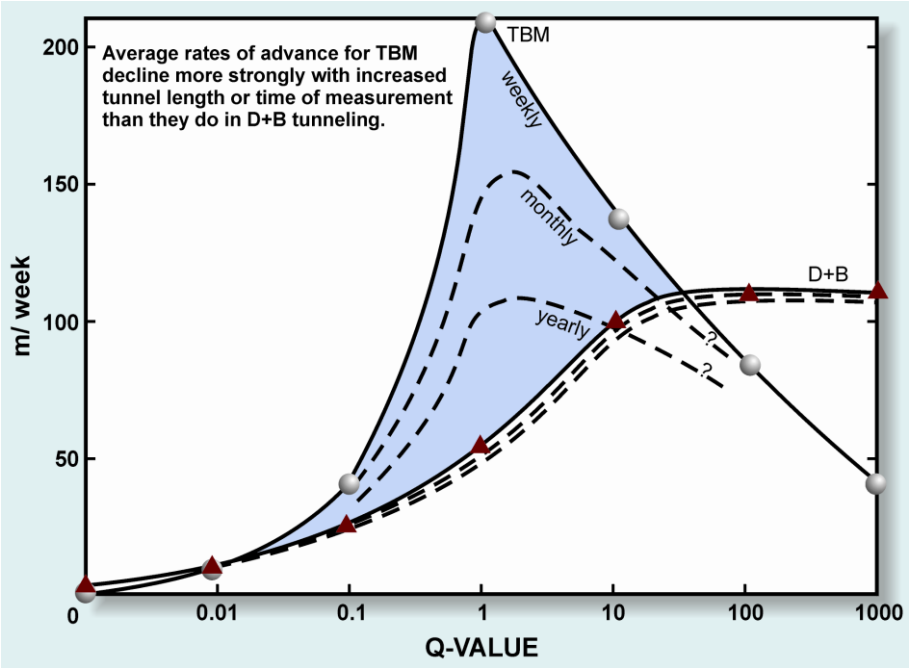

Figure 17. Comparing TBM and drill-and-blast in similar rockmasses, we see the need for a modified classification for TBM prognosis, and the effect of time is clearly 'adverse' for the TBM. The TBM is a supremely efficient method for 'central' rockmass qualities. (Barton, 2000).

Double-shield TBM for minimising minor geological delays

Use of double-shield TBM for PC-element building can solve minor stability problems without encountering significant delays, but when significant fault zones are intersected, the double-shield may actually represent a hindrance to rapid recovery, as pre-treatment of the ground ahead is hindered by the long shields.

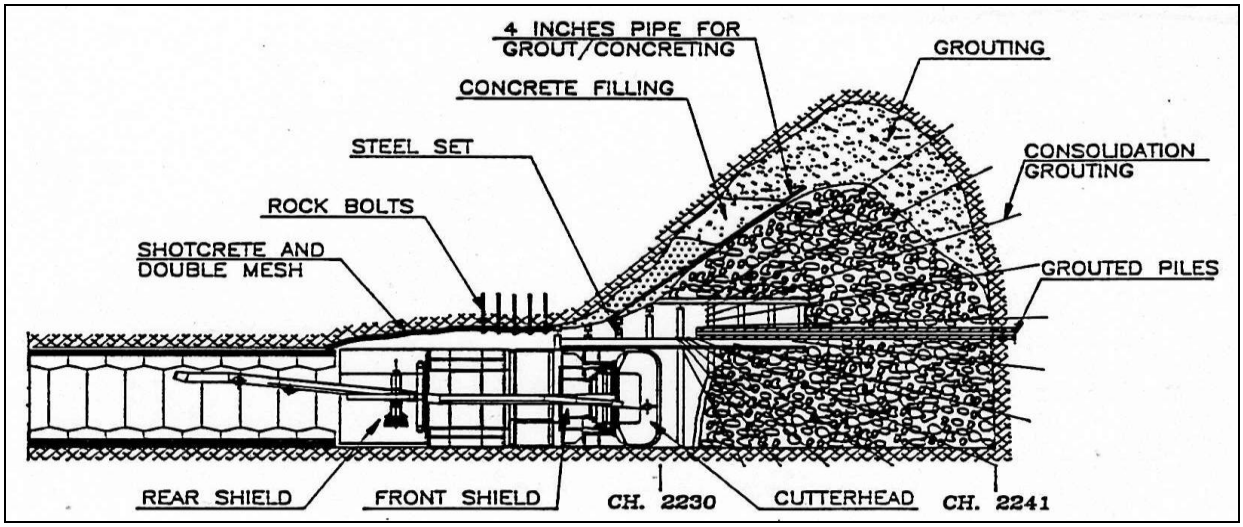

Figure 18. Detail from recovery operations described by Grandori et al. 1995. Despite the sophistication of double-shield operations (and their greater cost), hand-mining operations may be needed on occasion.

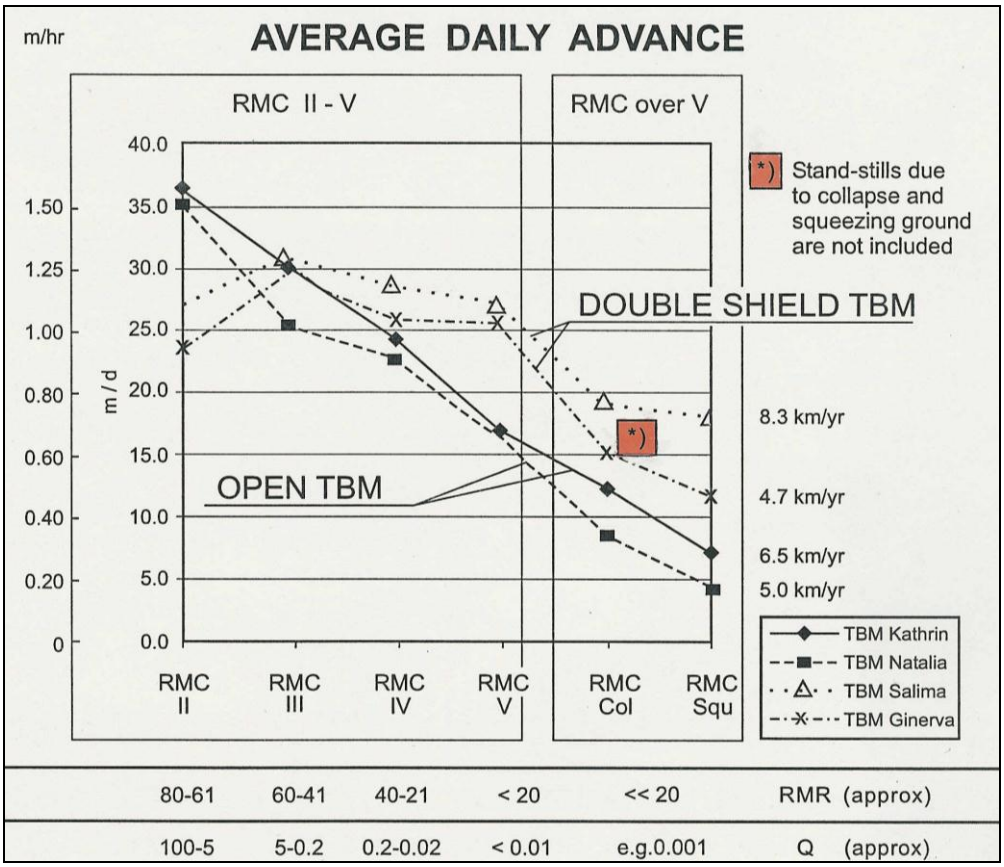

Figure 19. The Evinos-Mornos tunnel had two open TBM, and two double-shield TBM. Grandori et al.1995 gave this comparative performance data. Tentative RMR and Q scales have been added by Barton, 2000. Note that 'stand-stills' (i.e. caused by fault zones) are not included.

Figure 20. Photograph of a modern double-shield machine, one of four used at the Guadarama tunnels in Spain.

Figure 21. PC-elements assembled under the protection of the tail-shield, allow 'continuous' operation of the TBM when dimensioned to take the thrust while re-setting grippers. Guadarama, Spain.

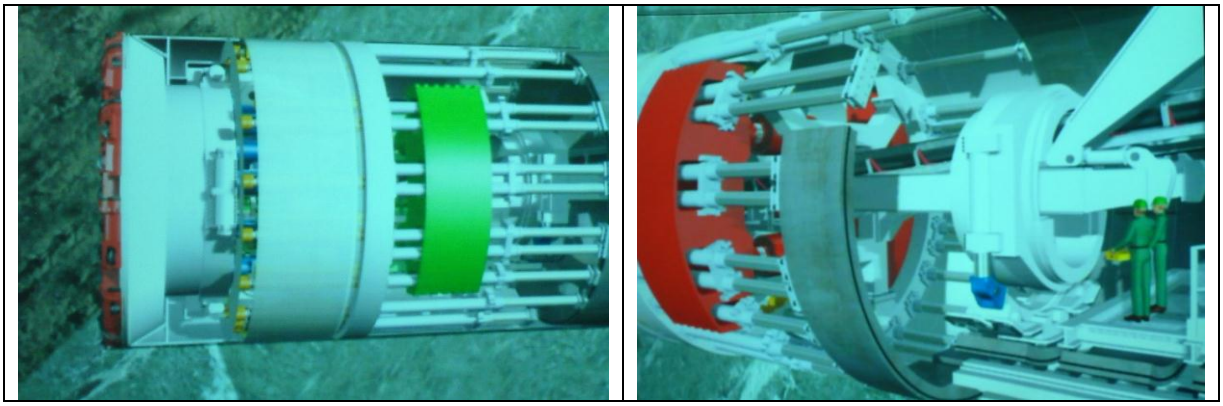

Figure 22. A computer animation of the 'continuity' of operations at Guadarama. Left shows thrust off PC-elements (with gripper re-set shown in green), right shows PC-element building during thrust off grippers (shown red).

Despite the hard massive granites and gneisses at Guadarama, and the need for frequent cutter change, the overall efficiency of the 'continuous' thrust abilities described above, allows for a very shallow (excellent) gradient of deceleration (-m), as demonstrated by hand-written comments in the Figure 23 Q_{TBM} model chart shown next.

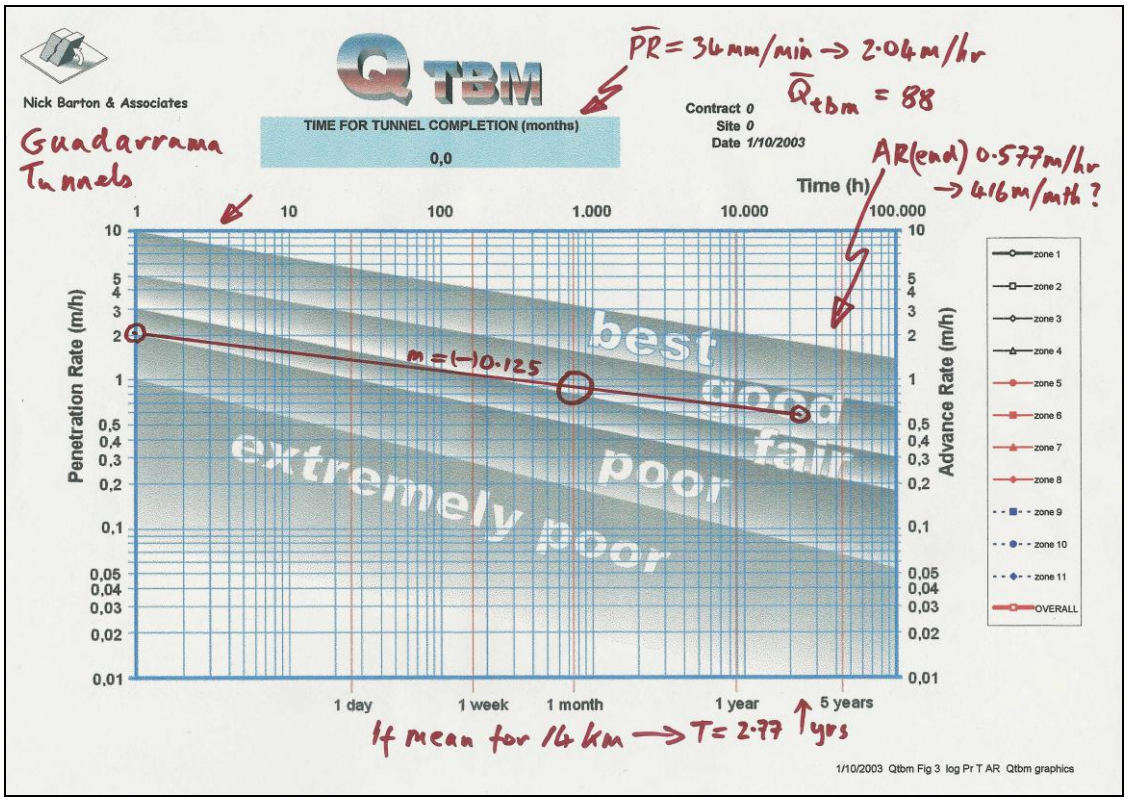

Figure 23. Despite frequent cutter changes, and a relatively low PR and therefore a high (unfavourable) Q_{TBM} value of 88 (see later), the high efficiency of 'continuous' boring at Guadarama gives an extremely small gradient of deceleration (-0.125), crossing 'normal' performance trends.

Figure 24. The price that one pays for this excavation efficiency is a huge materials fabrication and handling operation, at both portals if excavating from both ends.

TBM problems at Dul Hasti HEP in Kashmir

We will now move further east into the foothills of the Himalayas, and record an extreme water and pebble/sand blow-out, plus stand-up time problems in inter-bedded phyllites, mixed with PR rates as low as 0.2m/hr due to sections of massive abrasive quartzite.

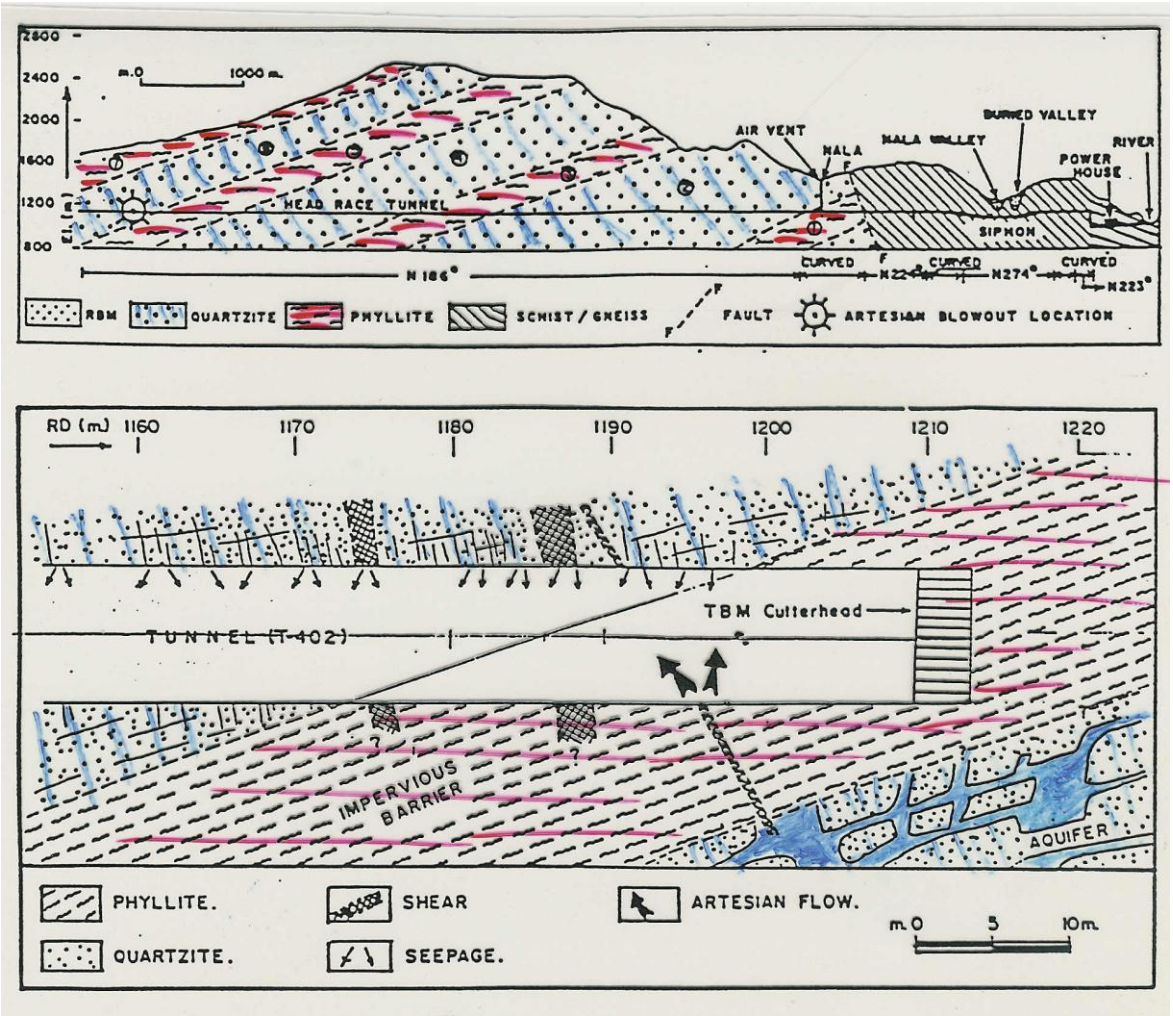

Figure 25. Simplified geology, and the location (ch. 1,215) of an extreme in-rush (or blow-out) of water, sand and rounded quartzite pebbles – at 750m depth, which originated in the invert and was therefore not detectable by 'conventional' forward-and-upward probe drilling (which nevertheless was absent). Deva et al. 1994.

The blow-out consisted of about 4,000 m^3 of sand and quartzite pebbles (partly rounded by sub-terrainian flow) that buried the TBM, and an initial $60m^3$/min water inrush, that subsequently required a separate drainage tunnel to the valley-side. There was talk of miners having escaped from the flooded/buried TBM by escaping above the water, inside the air-ventilation ducts.

The fractured quartzite 'aquifer', sandwiched between impermeable phyllites, had its surface exposure more than a kilometer above, and distant from the river valley. The connection of this 'aquifer' to the tunnel was by a minor shear, not even a fault.

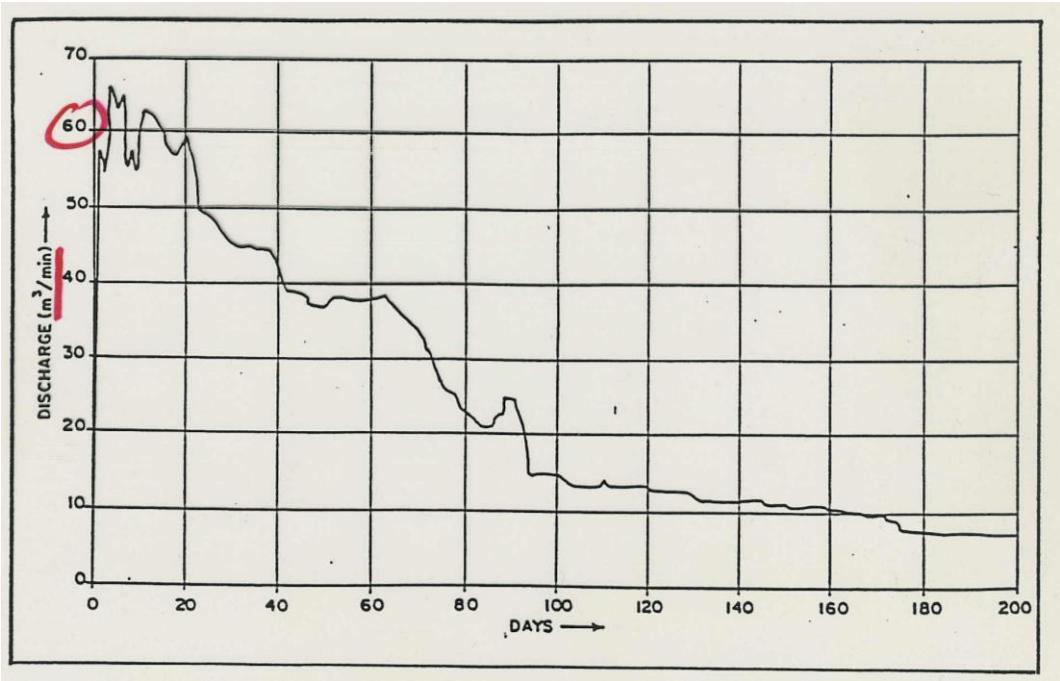

Figure 26. The initial 200 days of water in-inflow recordings that remained above 5 m^3/min even 5 years later. There was a 280 days delay due to this blow-out.

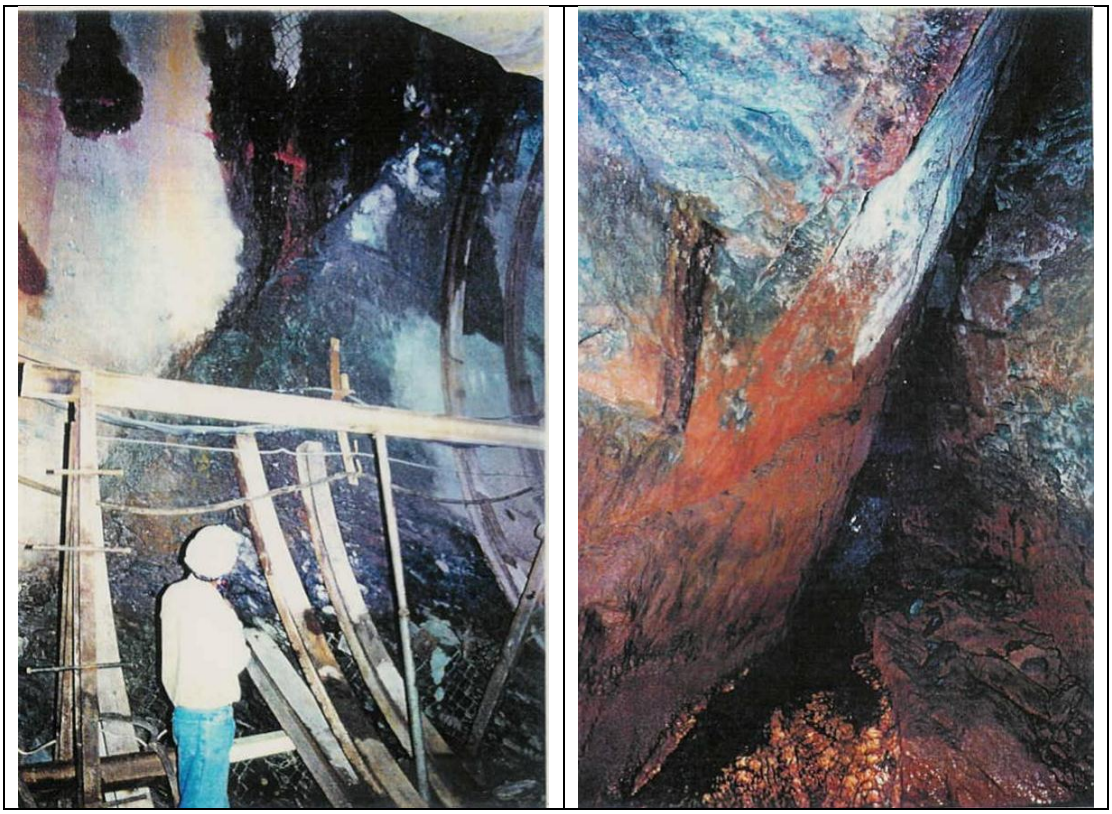

Figure 27. The location of the shear zone (left wall), and blow-out location (right wall / invert), as viewed some years after the event.

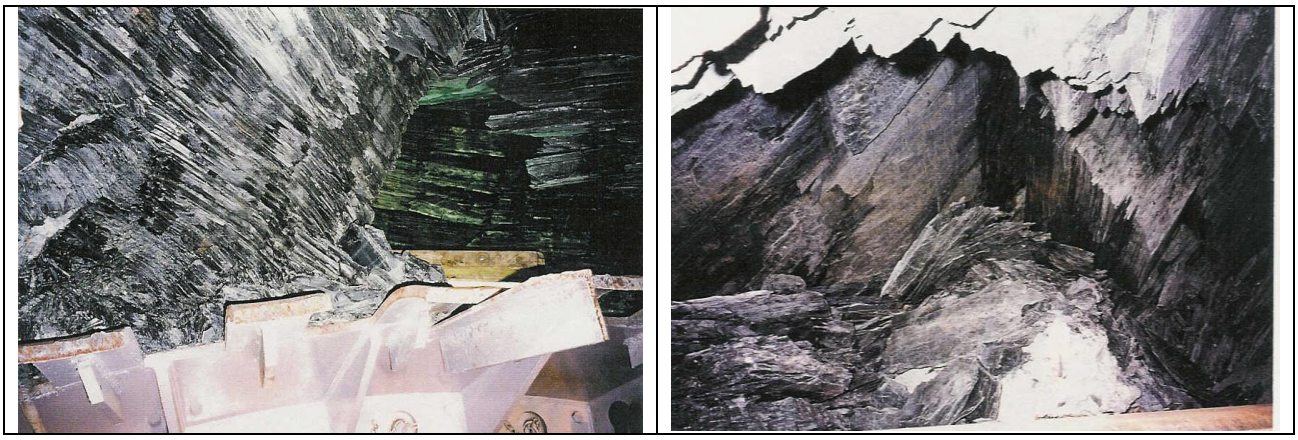

Figure 28. A subsequent location (around ch 1630) of stand-up time problems in sheared, talcy phyllites, where a void of 3 to 4m depth developed in the left wall, due to 'over-excavation' by the TBM, caused by the negligible stand-up time of this sheared rockmass.

Figure 29. A detailed view of the sheared phyllite next to the single shield TBM.

The sheard, talcy phyllite was difficult to walk on, behaving like dry bars of soap. Blocks continued to fall from the sheared left wall, while the arch was in quite massive phyllites.

Figure 30. The TBM had been excavating more material than (π $R^{2)}$ x length of advance, due to the stand-up time limitations of the sheared phyllites.

Figure 31. Block falls from the left wall continued during attempts to shore-up the void and back-fill with cement/sand sacks.

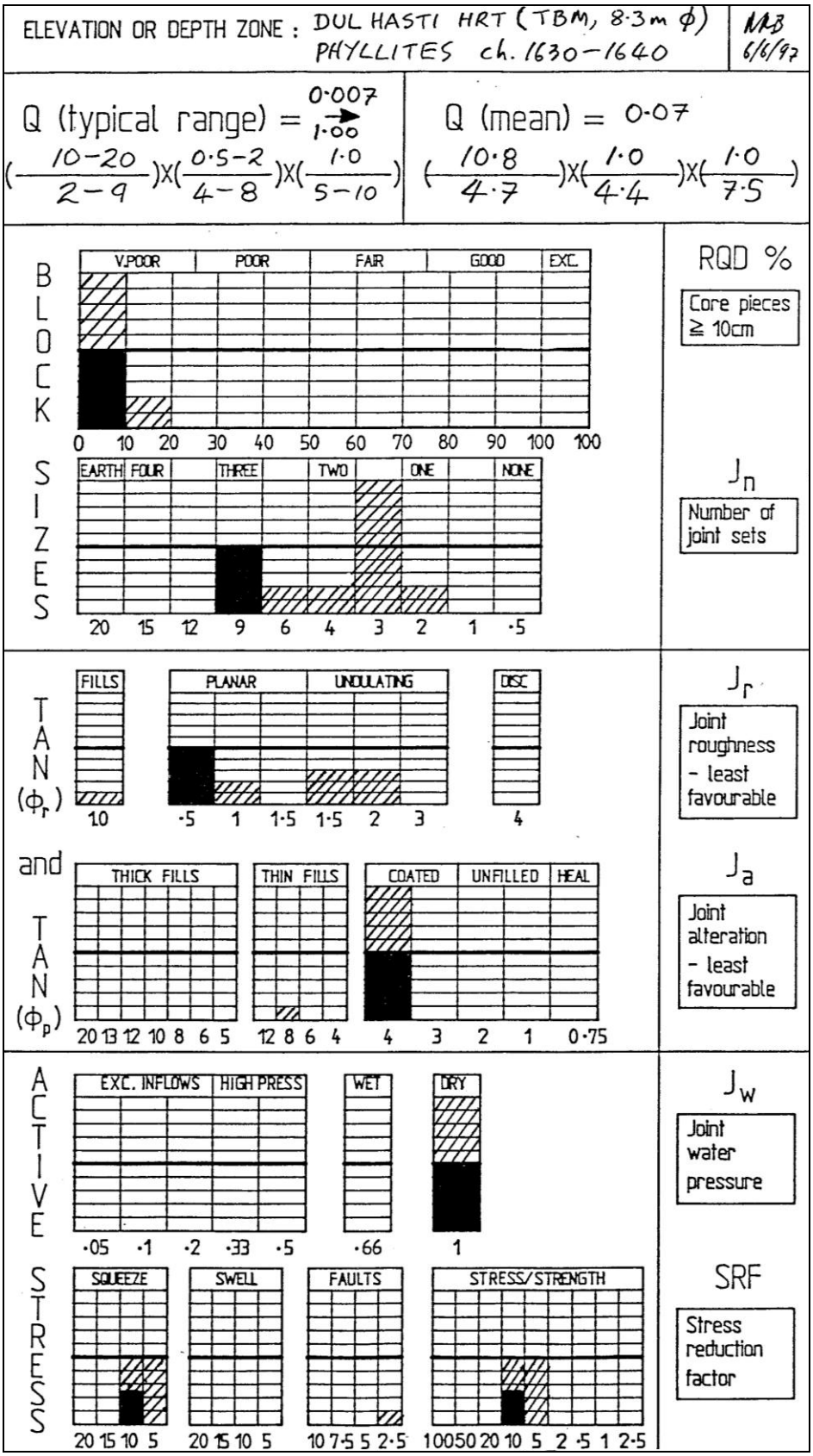

Figure 32. Q-parameter recordings in histogram format, for the sheared talcy phyllites illustrated previously. Note that due to contract re-negotiation, this TBM (abandoned by the original contractor) had progressed only 400m in about 4 years.

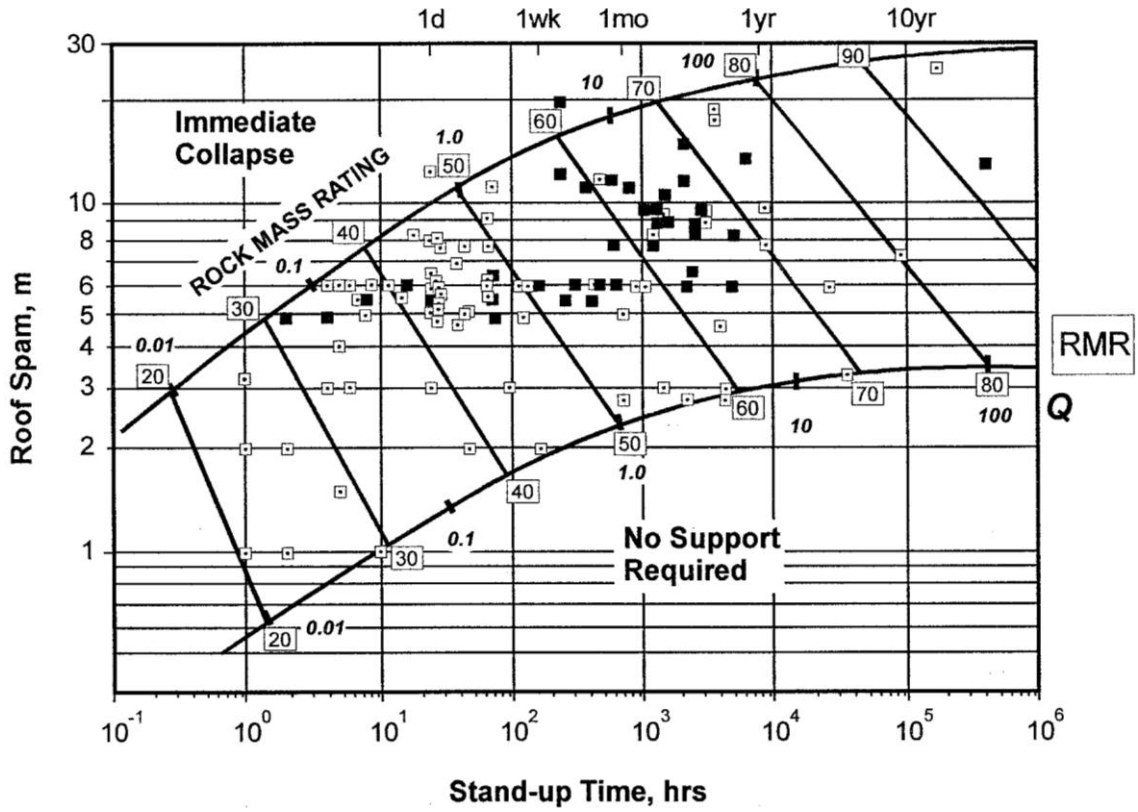

Figure 33. Stand-up time data plotted by Bieniawski, 1989, with RMR to Q conversion with the following equation from Barton, 1995.

The Q-parameter logging provided an estimate of Q_{mean} as follows:

Q_{mean} = 0.07 in the sheared phyllite

Assume RMR ≈ 15 log Q + 50 (Barton, 1995)

From Figure 33:

1m (without support) ≈ 1 hour stand-up,

5m (no support until finger shield) ≈ 0.1 hr stand-up

Borrowing the 'stand-up' time and 'roof span' data of Bieniawski 1989, we therefore find that the predicted stand-up time for an unsupported span (measured from last support) can have these adverse (much too short) magnitudes. These values easily explain why the TBM cutter-head was able to 'over-excavate'.

Fault related problems at SSDS Tunnel F in Hong Kong

The Tunnel F problems were mostly related with fault zones, and with the difficulty of pre-injection in a small-diameter TBM tunnel. This particular contract was completed by Skanska International, following re-negotiation of all the contracts after the withdrawal of the original contractor. The tunnel is in the top-left corner, going sub-sea, some 3km from Tsing Yi Island to Stone Cutters Island, and underneath the world's second largest container port.

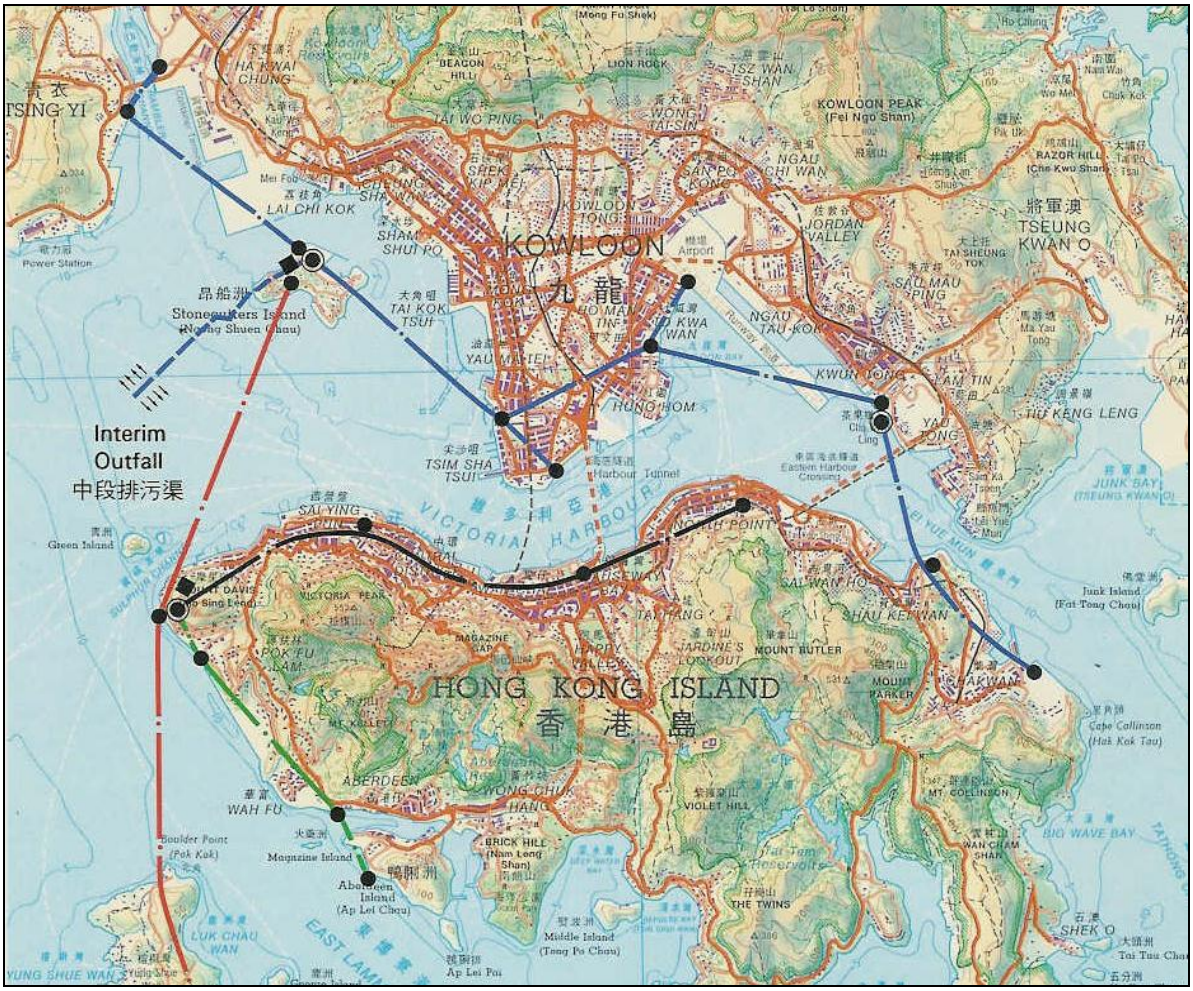

Figure 34. The Strategic Sewage Disposal System (initial TBM tunnels are nearer the Kowloon side of Hong Kong harbour). Much of the NE harbour area is now reclaimed land.

Unfortunately, the tunnelling contract consultants failed to detect and locate a major regional fault zone: the Tolo Channel fault zone, due in part to the difficulty of performing the sub-sea seismic profiling exactly as intended. Due to intense shipping activity close to the container port the seismic velocity profiles did not succeed in extending into the low velocity areas.

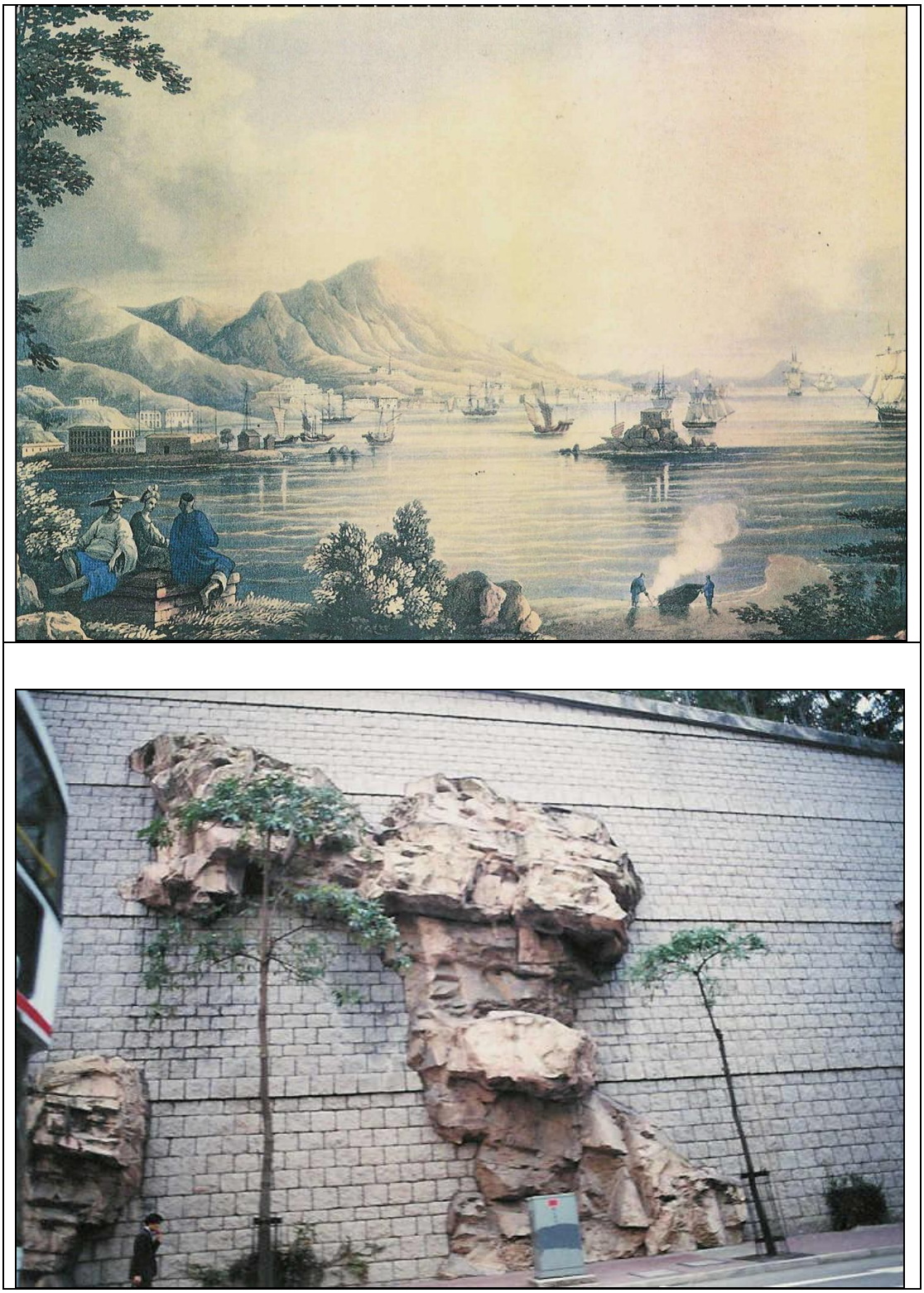

Figure 35. The present intensely developed urban area of Kowloon and Hong Kong (with rare untreated exposed rock now preserved in places as 'architecture'), contrasts greatly with the geologist's possibilities of surface mapping in previous centuries. Today, smaller-scale features of the rock mass can be (temporarily) seen in cuttings, while large scale features of the terrain are largely obscured.

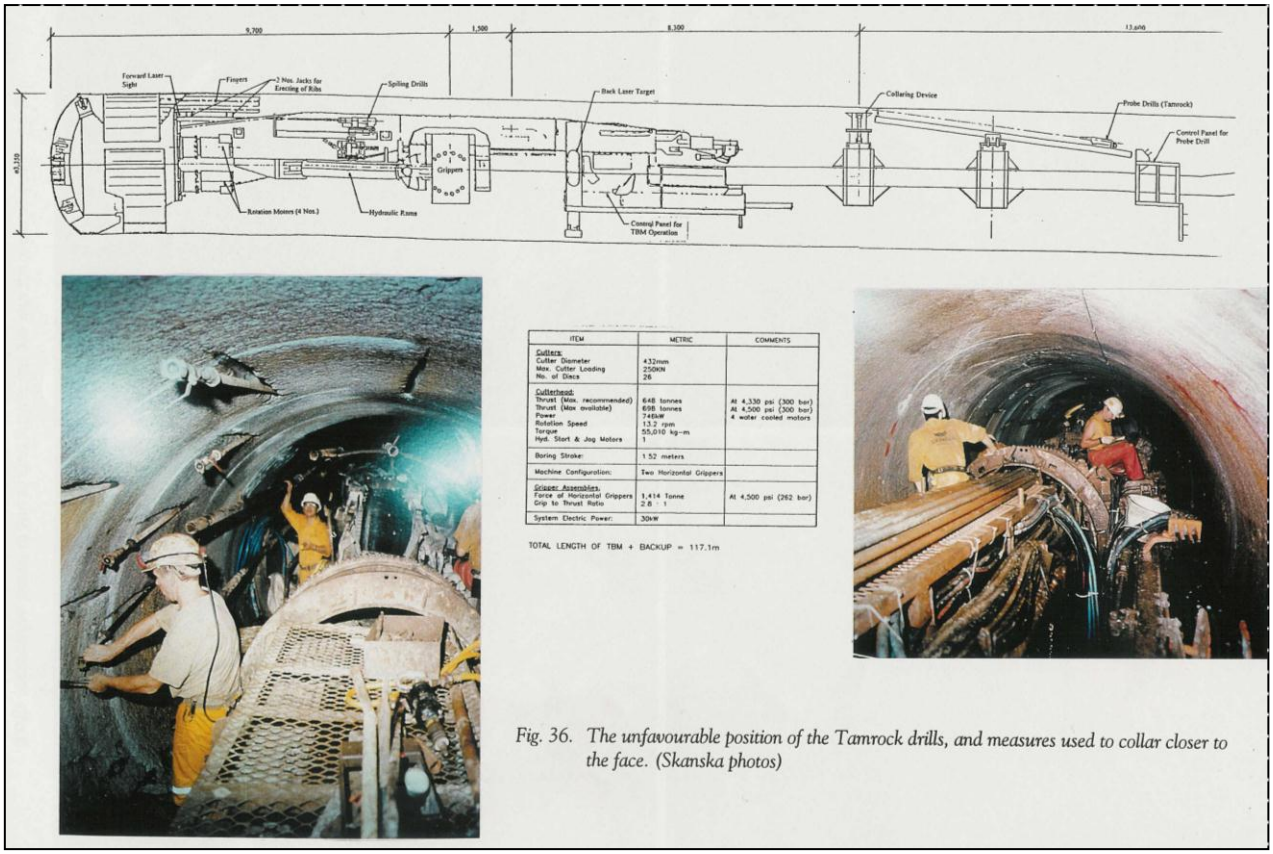

ITEM	METRIC	COMMENTS
Cutters: Cutter Diameter Max. Cutter Loading No. of Discs	432mm 250KN 26	
Cutterhead: Thrust (Max. recommended) Thrust (Max available) Power Rotation Speed Torque Hyd. Start & Jog Motors	648 tonnes 698 tonnes 746kW 13.2 rpm 55,010 kg-m 1	At 4,330 psi (300 bar) At 4,500 psi (300 bar) 4 water cooled motors
Boring Stroke:	1.52 meters	
Machine Configuration:	Two Horizontal Grippers	
Gripper Assemblies: Force of Horizontal Grippers Grip to Thrust Ratio	1,414 Tonne 2.8 : 1	At 4,500 psi (262 bar)
System Electric Power:	30kW	

TOTAL LENGTH OF TBM + BACKUP = 117.1m

Fig. 36. The unfavourable position of the Tamrock drills, and measures used to collar closer to the face. (Skanska photos)

Figure 36. The confined conditions for performing pre-injection (Skanska photos).

Figure 37. With inflows as high as 1m^3/sec locally, and huge quantities of grout, and several serious stability problems, an important aspect was worker morale - and drying of clothes between shifts.

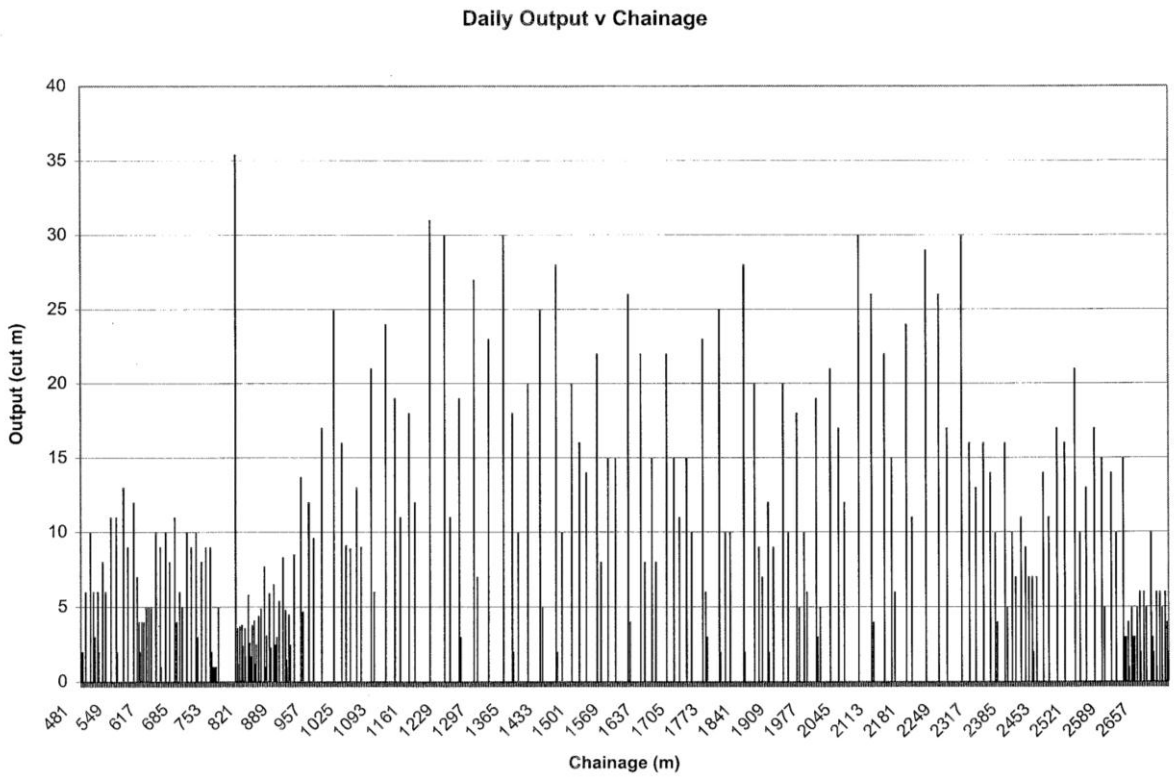

Figure 38. Daily advance versus chainage, from beginning of Skanska project (ch.481) to time of consultant's visit. The 'dark' areas are fault zones, or where particular water control problems were experienced.(Skanska data).

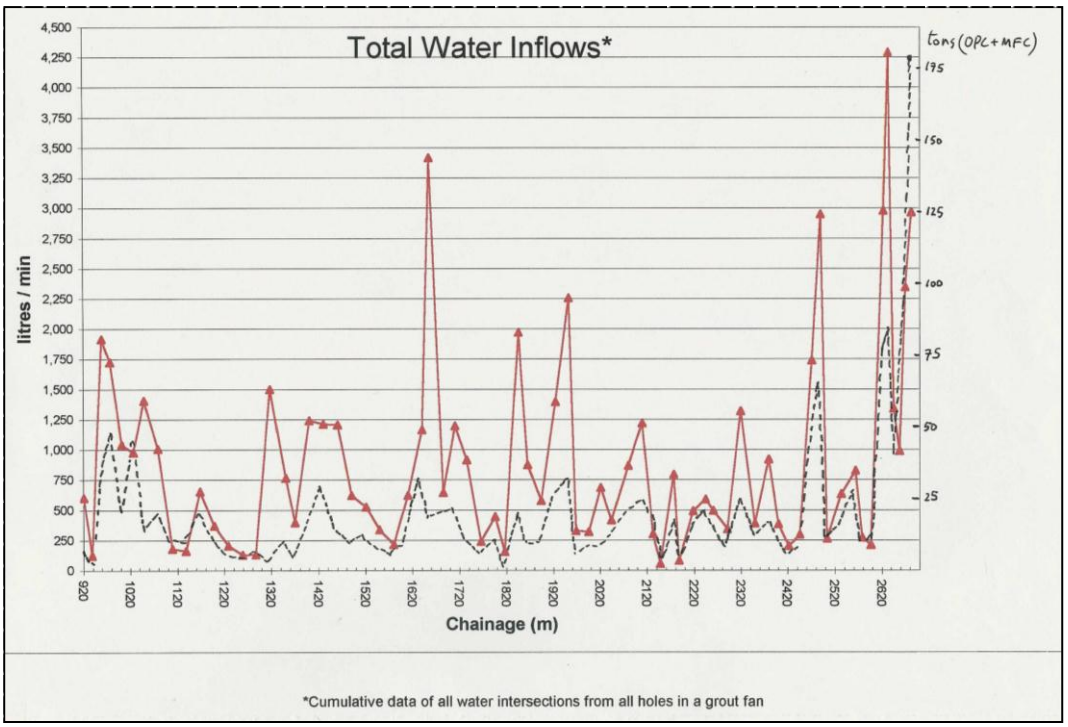

Figure 39. Super-imposed water inflows (cumulative, all holes) and OPC+MFC grout take (dotted lines), show general correlation. (Skanska data).

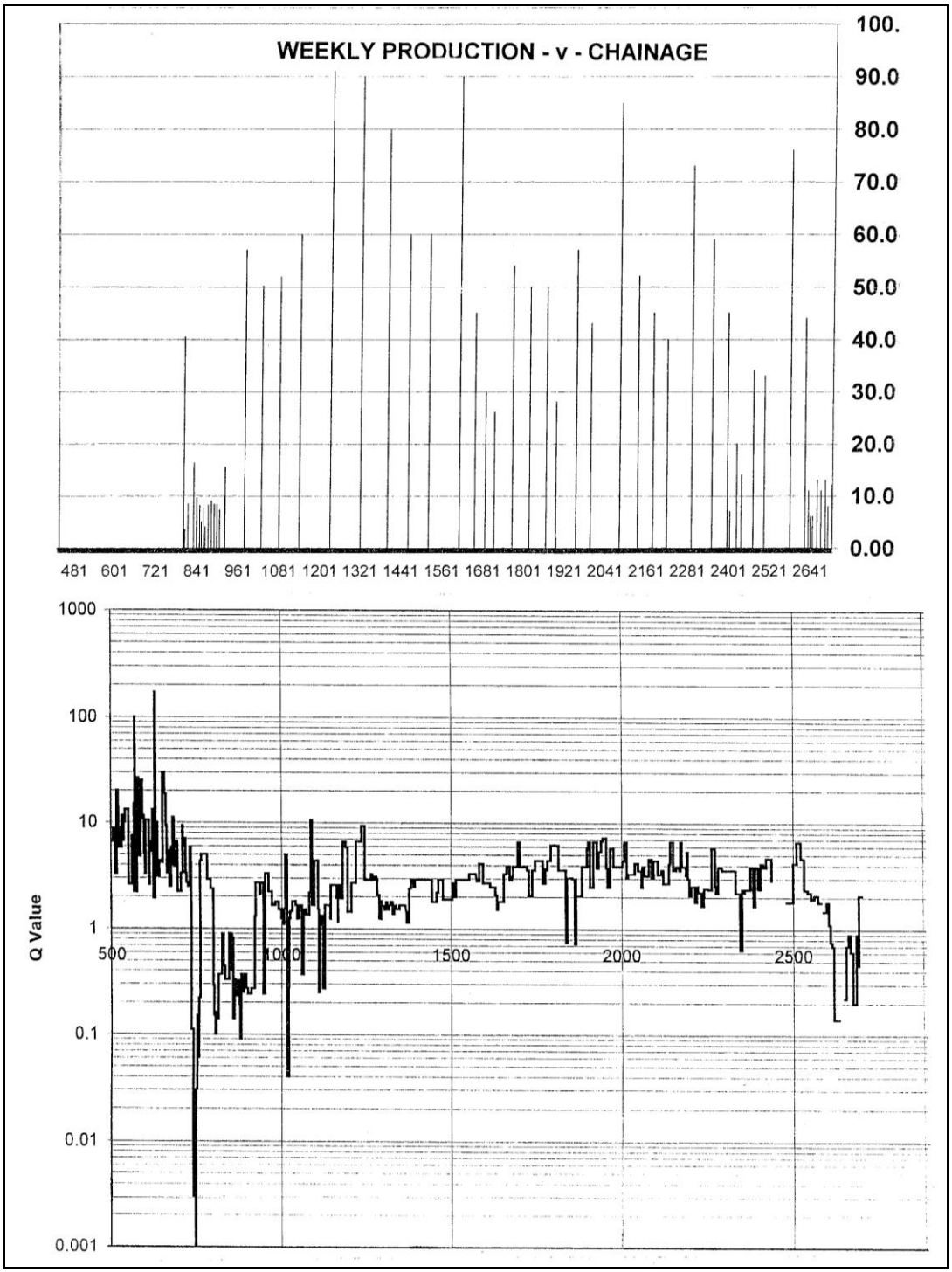

Figure 40. Correlation of logged Q-values and weekly advance, which was below 10m/week on numerous occasions due to faulting and water control delays. (Skanska data).

A summary of the situation at Tunnel F (when the author visited the tunnel for the first time was as follows):

- 481m of the tunnel was completed in a previous project

- 3098m remained for the new contractor (Skanska)

- The Owner/Consultant expected 96m/week, 204m/week and 228m/week (in poor, fair and good rock conditions – with a TBM inherited from the previous contractor)

- The conforming contract demanded 1 year for completion (of 3098m)

- During 29 months, 2221m of new tunnel was driven by Skanska

- This represented an AR of 17m/week (or AR=0.1m/hour) – which was 1/10 of the Owner/Consultant general expectation (and 1/3 of the conforming contract)

- Chainage 744-759 (15m) had taken 8 months due to the need for hand-mining a by-pass round the stuck TBM in the first major fault zone (this represents a major 'unexpected event' with AR=0.003m/hour – and a mapped Q-value of about 0.001)

- Ch. 2622-2702 (80m) took 4 months and 750,000kg of grout (average AR= 0.03m/hr, i.e. also like an 'unexpected event', as plotted earlier)

- 887m of tunnelling remained when the author started advising Skanska in 1999

- There was a major regional (Tolo Channel) fault zone ahead, which had not been drilled or seismically profiled, due to heavy shipping traffic

- Skanska decided to drill a long horizontal 'pilot hole' *backwards* from the shaft on Stonecutter's Island, to try to sample this major fault zone

- The hole went only 731m, as it was stopped by the Tolo Channel fault zone – despite three attempts at hole deviation

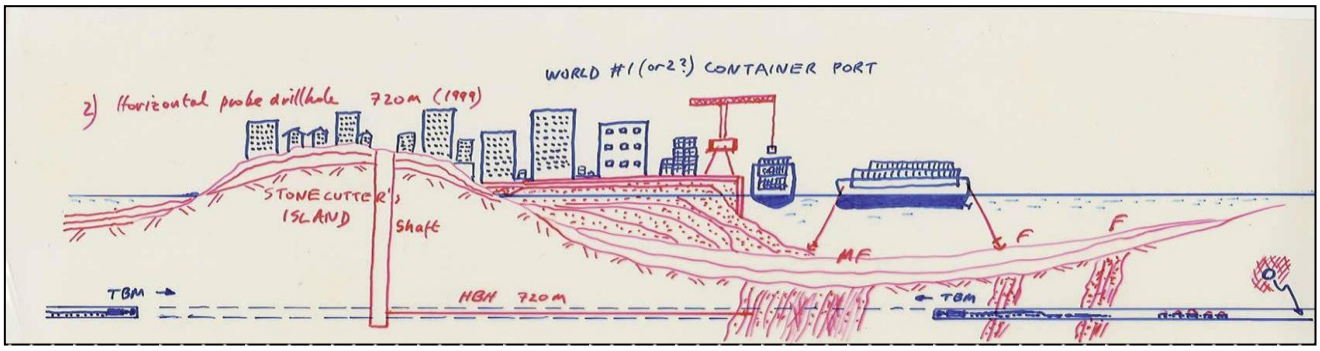

Figure 41. The remaining 887m of TBM-driven tunnel included the unexplored Tolo Channel fault zone. Only a few meters of this could be cored from the shaft location, yet the TBM later managed to penetrate the fault zone due to the pre-grouting effect on the rock mass. (NB sketch of situation in 1999).

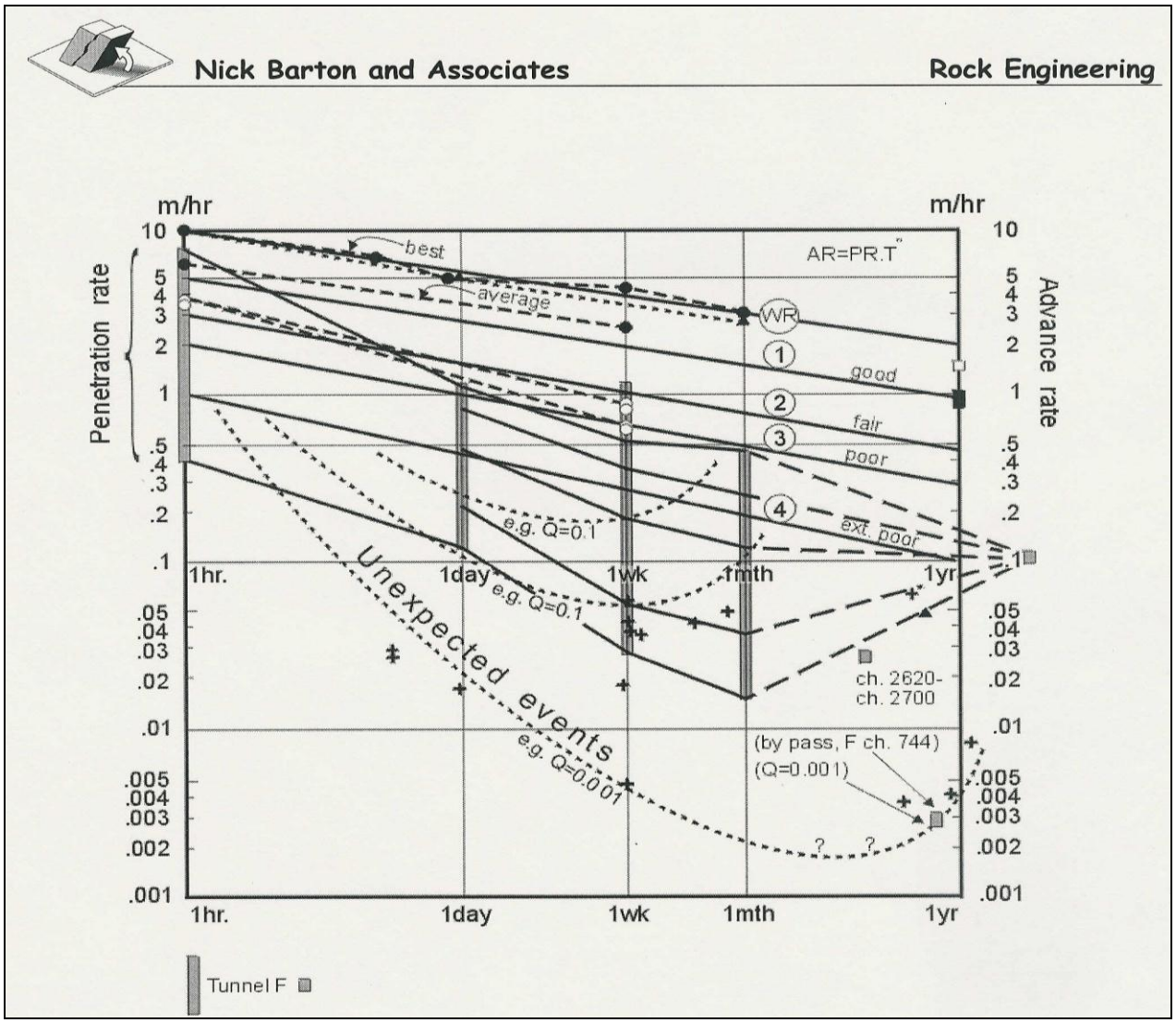

Figure 42. A plot of the recorded PR and AR performances of Tunnel F, superimposed on the Q_{TBM} chart of logPR – logAR – logT .

Analysis of pilot borehole (LH 01) core qualities for input to Q_{TBM} model

The 731 m of core recovered from the pilot hole sketched in Figure 41, provided Q-value input for much of the remaining tunnelling. The core was divided into five classes for convenience of description:

M = massive
S = slightly jointed
J = jointed
Z = zone (weathered)
F = fault

Photographs showing these five classes are reproduced in Figure 43.

Figure 43. Photographs of the five selected rock classes which, when Q-parameter logged, gave the approximate statistical frequencies of these five classes.

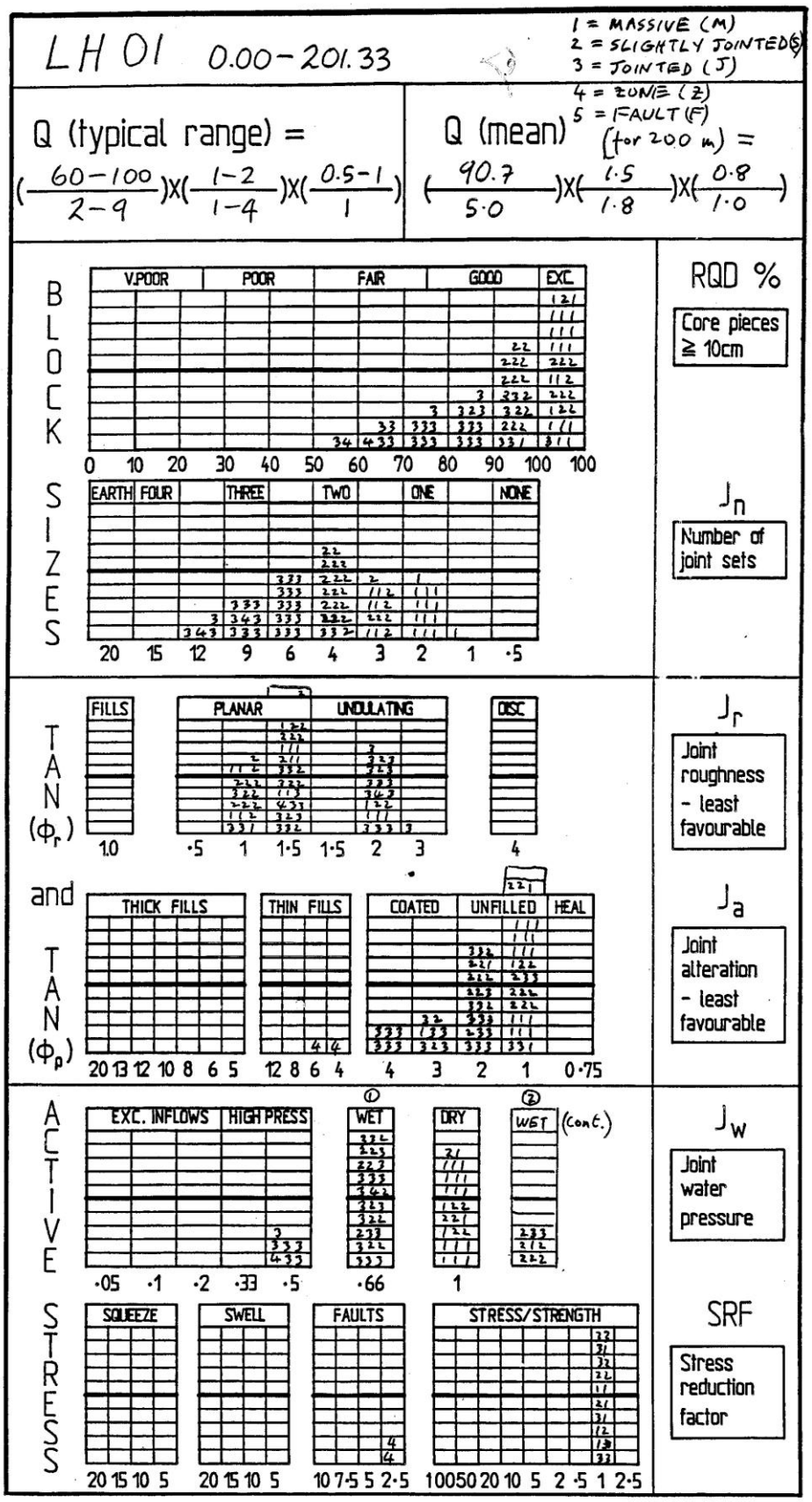

Figure 44. Q-parameter histogram logging of frequency of occurrence and ratings for the five rock classes, in the first 200m of hole LH 01 (i.e. the last 200m of the tunnel). (Note numbers 1 to 5 in each histogram, corresponding to rock class).

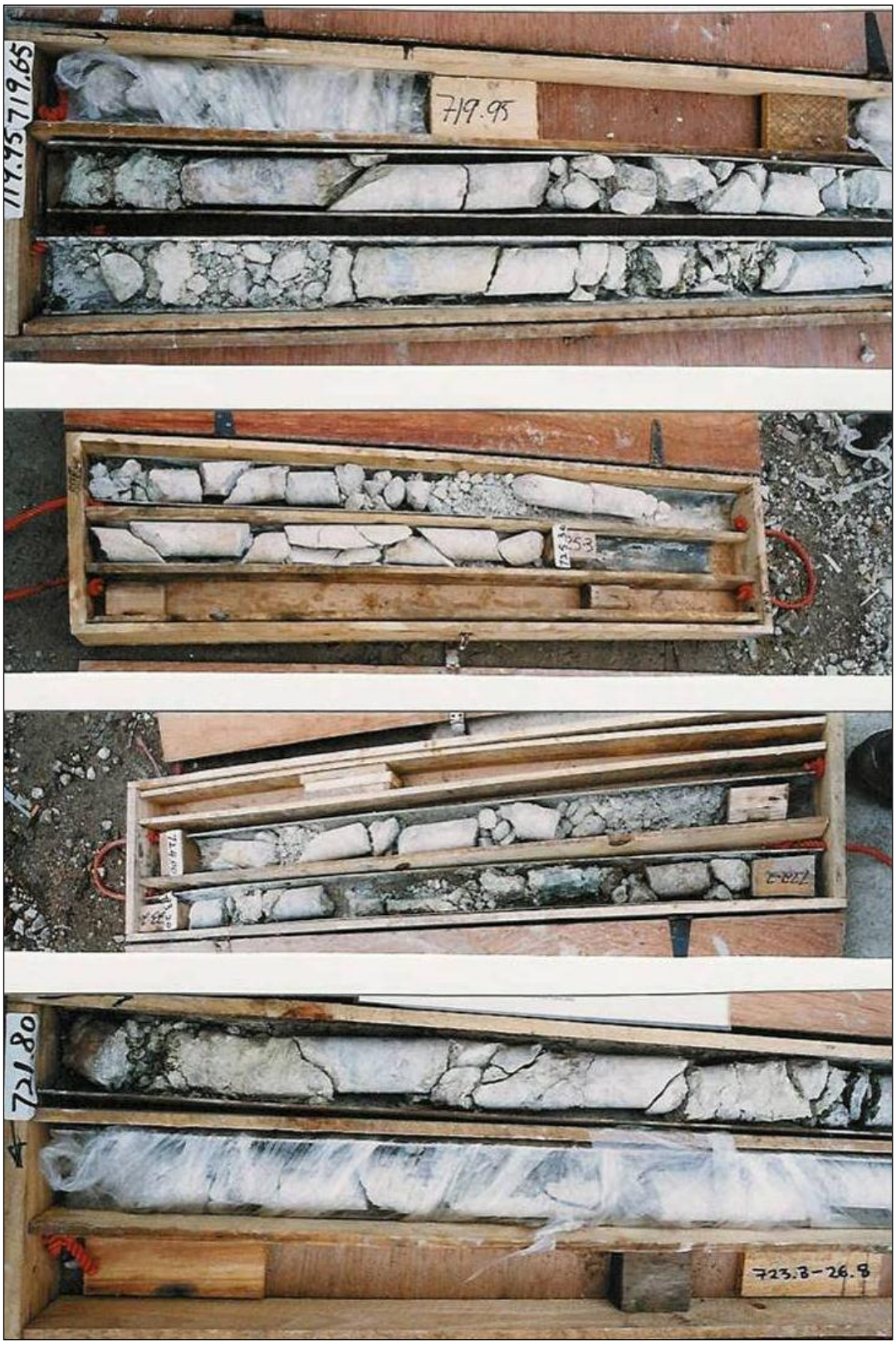

Figure 45. Three attempts were made to (deviate) drill into the Tolo Channel Fault Zone. These are the results - from the end of the 720m long horizontal pilot hole.

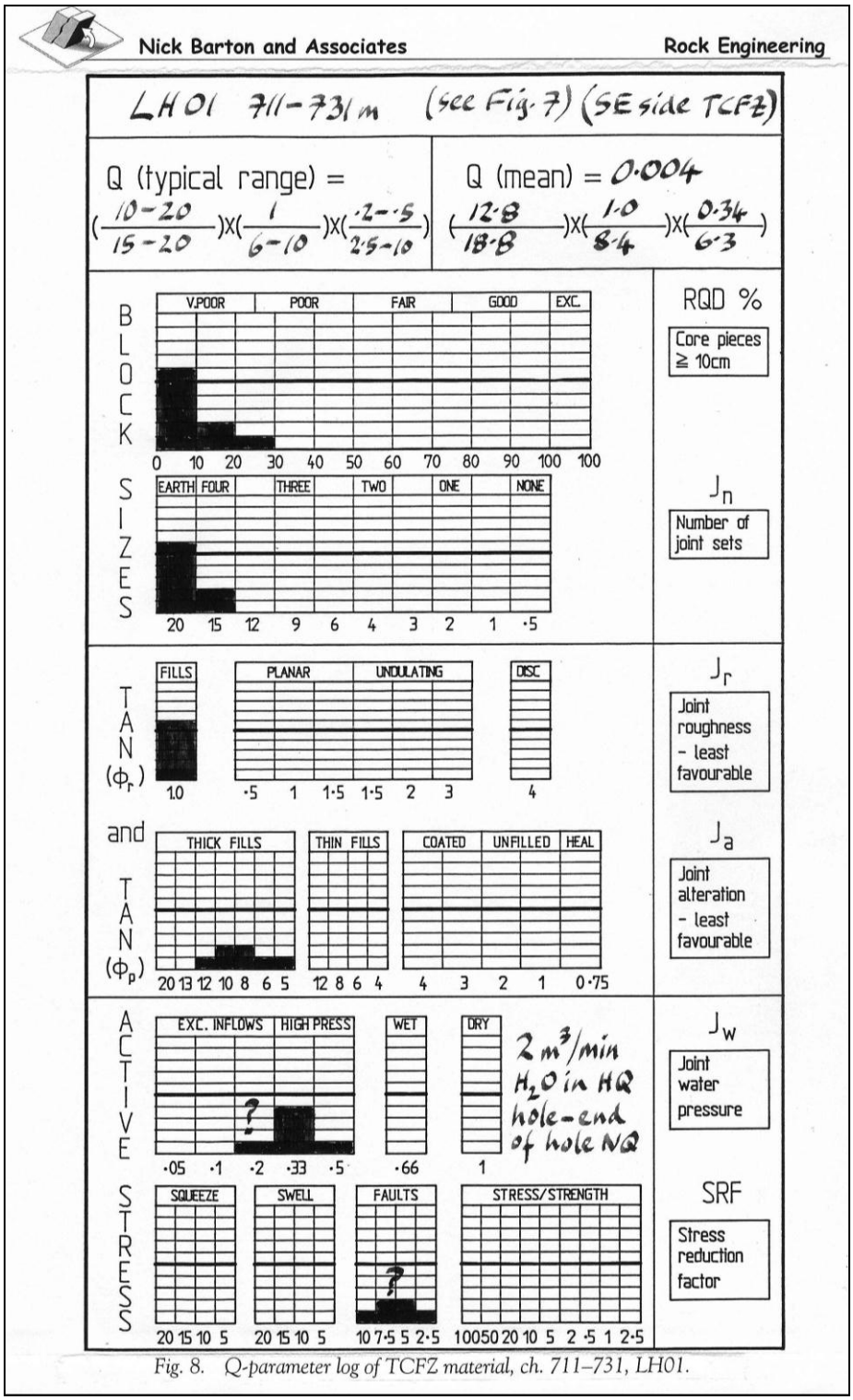

Figure 46. The Q-parameter characteristics of the fault zone (all that could be sampled) all plot 'to the left'. Q_{mean} = 0.004, i.e. needs improvement by pre-grouting

As shown in the next two figures, the availability of horizontal core data i.e. *parallel to the tunnelling direction,* is actually fundamental to a good TBM prognosis, especially when there is a marked anisotropy of structure.

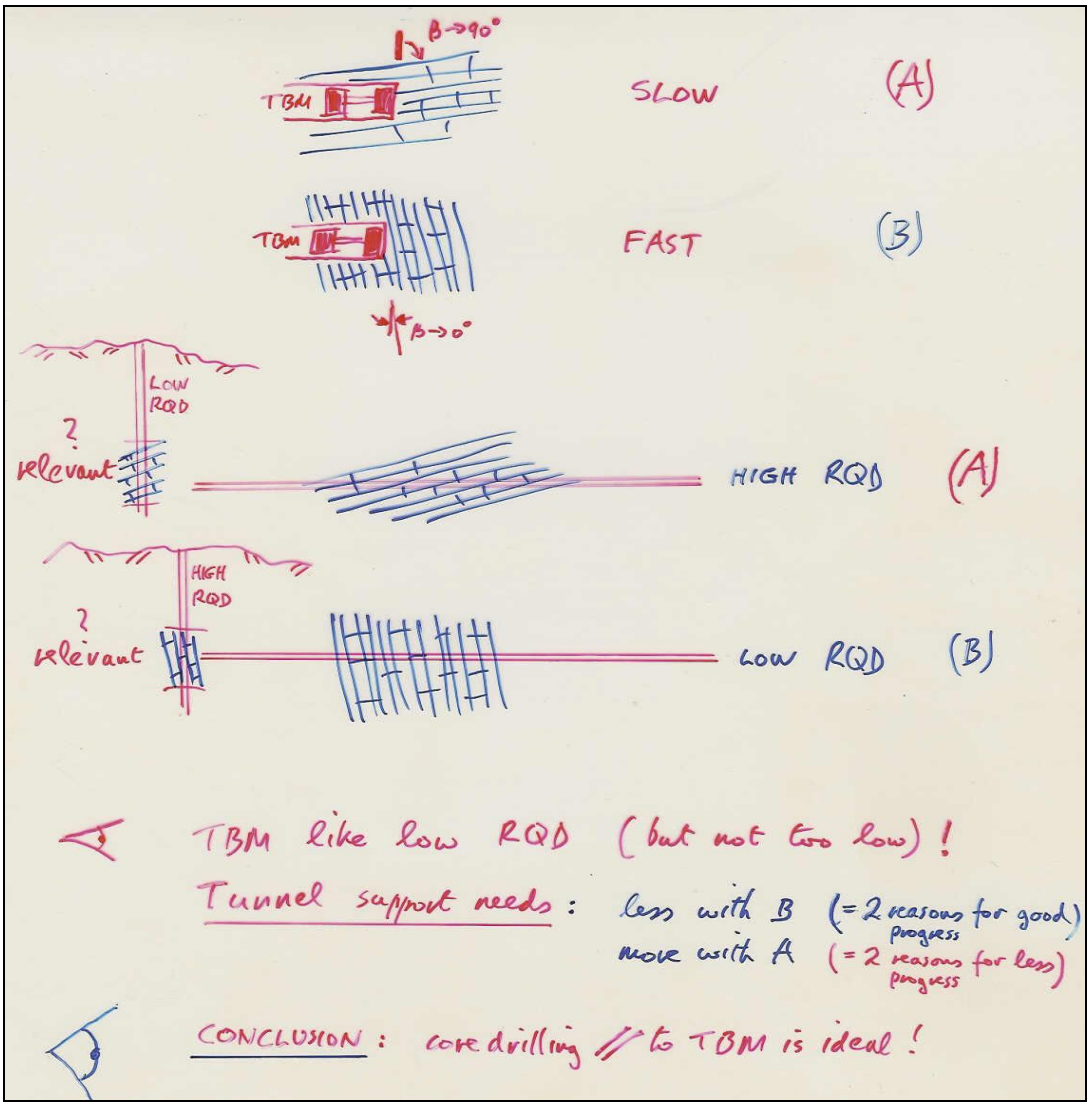

Figure 47. Sketches to demonstrate that horizontal boreholes (and therefore analysis of horisontal core) is the correct way to gather information for TBM prognoses when anisotropy of structure (bedding, foliation, schistocity, dominant jointing) is marked.

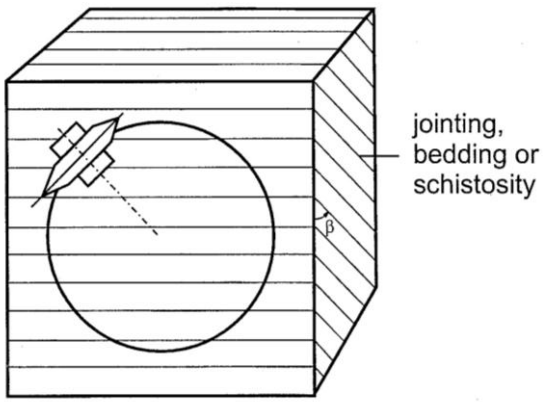

Figure 48. Ideal orientation of structure for best TBM penetration rate and advance rate (due to minimised support needs) is when angle β is small. Worst is when it is closer to 90º, as more rock has to be broken, without so much assistance from the existing structure.

While discussing horizontal core, it is appropriate to emphasise that ***if*** an efficient way of (multiple-hole) probe drilling and real-time analysis could be devised, for continuous application ahead of TBM, then operators could be better prepared for the changes that sometimes constitute serious 'unexpected events'.

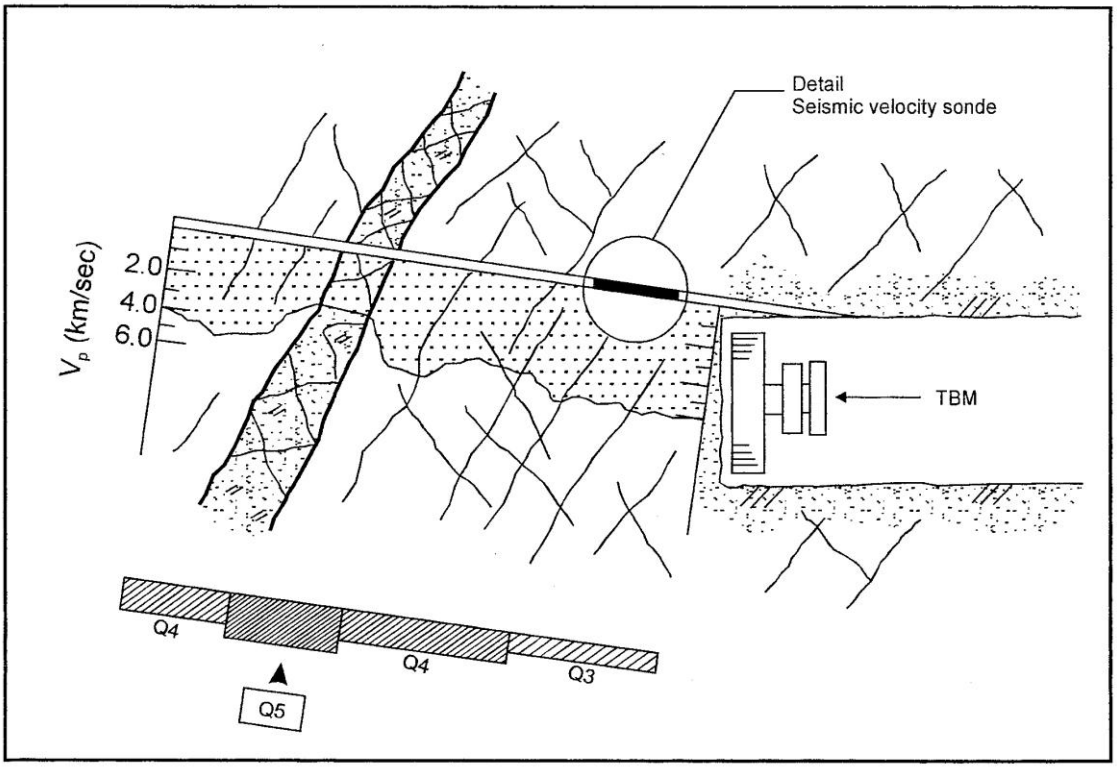

Figure 49. Conceptual use of probe holes for seismic logging ahead of TBM, and derivation of real-time information on e.g. the approaching Q-values, and perhaps need for pre-injection – not only for water control, but also for improving rockmass conditions.

Use of Q_{TBM} prognosis at Tunnel F based on core analysis

Three scenarios were modelled with the core data obtained from Q-logging of the horizontal core:

- FIRST, WITH NO PRE-GROUTING IMPROVEMENT
- SECONDLY, WITH GROUT-IMPROVED ROCK MASS….NET BORING TIME
- THIRDLY, WITH THE PRE-GROUTING CYCLE TIME (APPROX.) INCLUDED

Improvements in the rockmass properties caused by pre-grouting were based on the following types of arguments for particular rock classes: following Barton 2002.

RQD increases e.g. 30 to 50%
J_n reduces e.g. 9 to 6

J_r increases e.g. 1 to 2 (due to sealing of most of set #1)
J_a reduces e.g. 2 to 1 (due to sealing of most of set #1)

J_w increases e.g. 0.5 to 1
SRF unchanged e.g.1.0 to 1.0

Before pre-grouting *Q= 30/9 x 1/2 x 0.5/1 = 0.8*

After pre-grouting Q = 50/6 x 2/1 x 1/1 = 17

With similar improvements in the different rock classes, due to appropriate assumptions, following recommendations in Barton, 2002, there is a reasonable expectation of improving rock mass properties through the pre-grouting that was an almost standard procedure ahead of the TBM.

Table 1. Example of rock mass and tunnelling improvements that might be achieved by pre-injection. In poorer quality rock masses there could be greater improvements, in better quality rock masses it may be unnecessary to pre-grout.

Before pre-grouting	After pre-grouting
Q = 0.8 (very poor)	Q = 16.7 (good)
Q_c = 0.4	Q_c = 8.3
V_p = 3.1 km/s	V_p = 4.4 km/s
E_{mass} = 7 GPa	E_{mass} = 20 GPa
B 1.6m c/c	B 2.4m c/c
S(fr) 10 cm	none

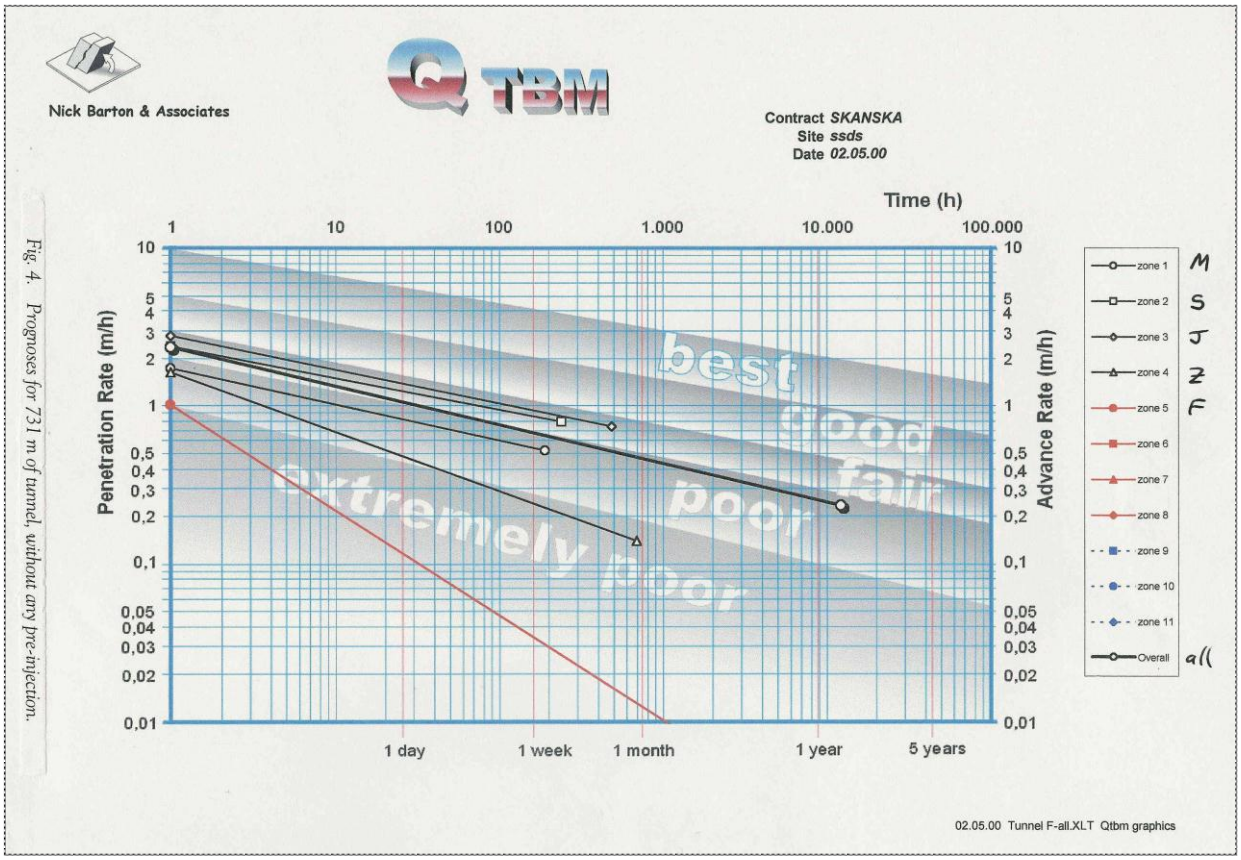

Fig. 4. Prognoses for 731 m of tunnel, without any pre-injection.

Figure 50. No pre-grouting improvements….more than 1 year needed.

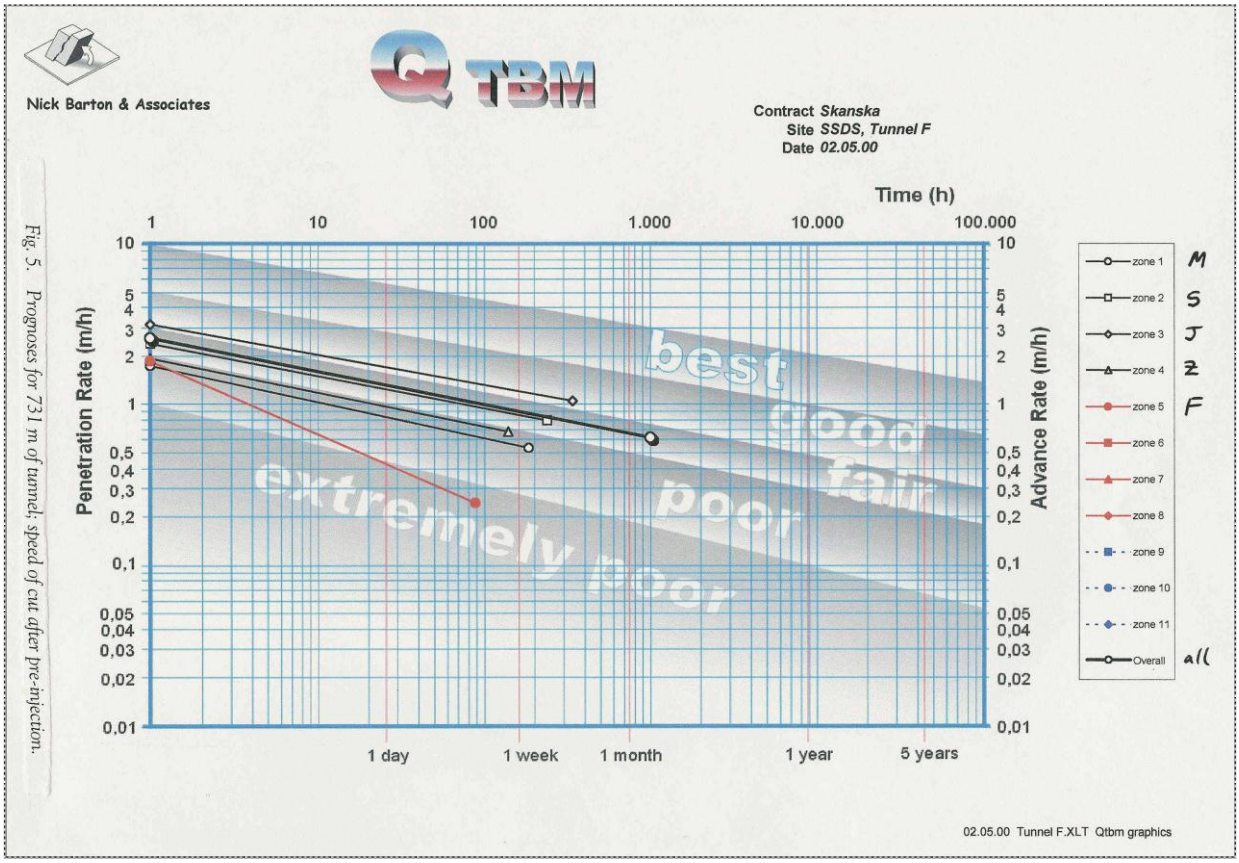

Fig. 5. Prognoses for 731 m of tunnel; speed of cut after pre-injection.

Figure 51. Net boring time with pre-grouting improvement. Note reduced gradients.

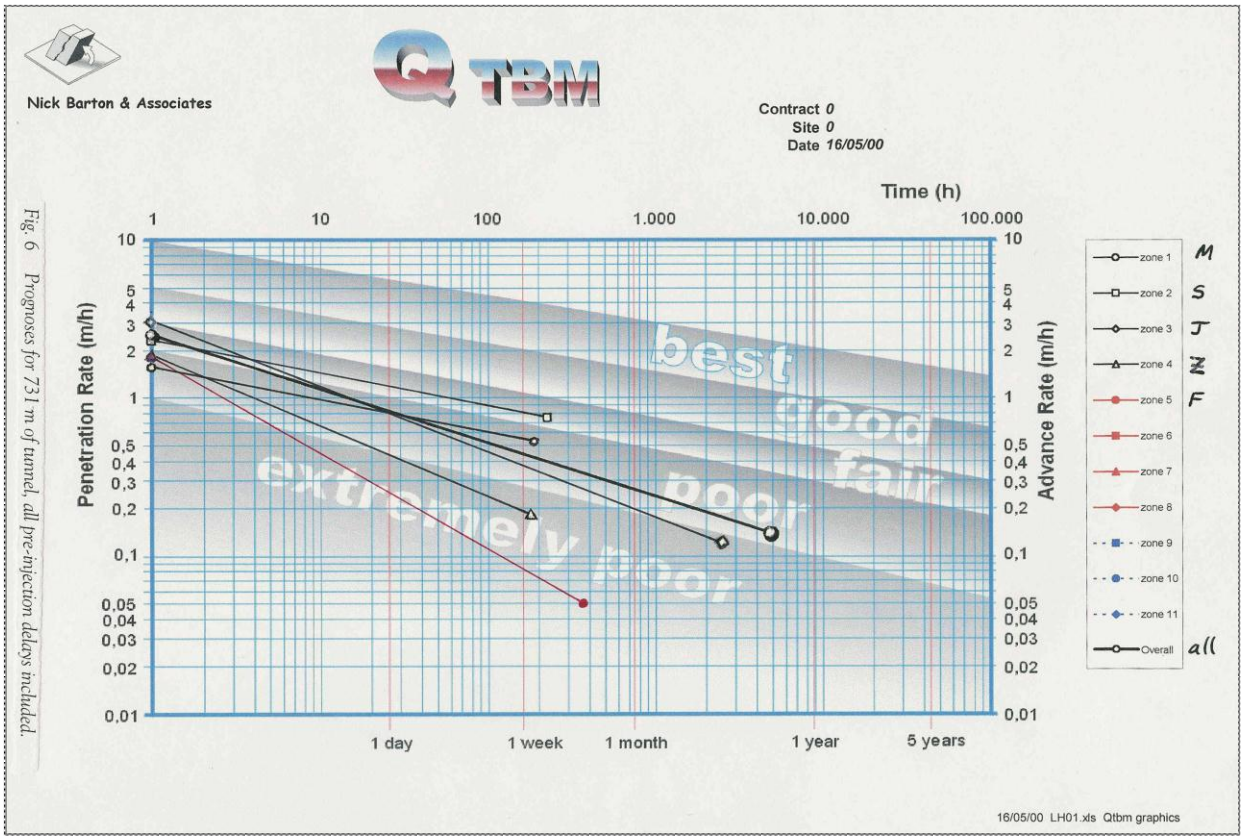

Figure 52. Total tunnelling time with pre-grout cycles (two estimates). Actual time was 2 months for the last 700m. (Total time for Skanska's 3097m was 37 months)

The following is a summary of the results obtained with the Q_{TBM} modelling predictions:

<u>ZONES M, S, J, Z (**m**assive, **s**lightly jointed, **j**ointed, weathered **z**one)</u>

L = 710m, 19 weeks ***with*** pre-injection (needed for water control)

L = 710m, 6.2 weeks ***without*** pre-injection

<u>ZONE F (**f**ault zone)</u>

L = 21m, 2.3 weeks ***with*** (successful) pre-injection

L = 21m, **1.4 years *without*** pre-injection

The author's prediction for 3097m remaining tunnel (following 2270m known) was a total of 3.5 years. Actual completion was 37 months or 3.1 years. The pre-injection performed by Skanska had perhaps an even more beneficial result than assumed

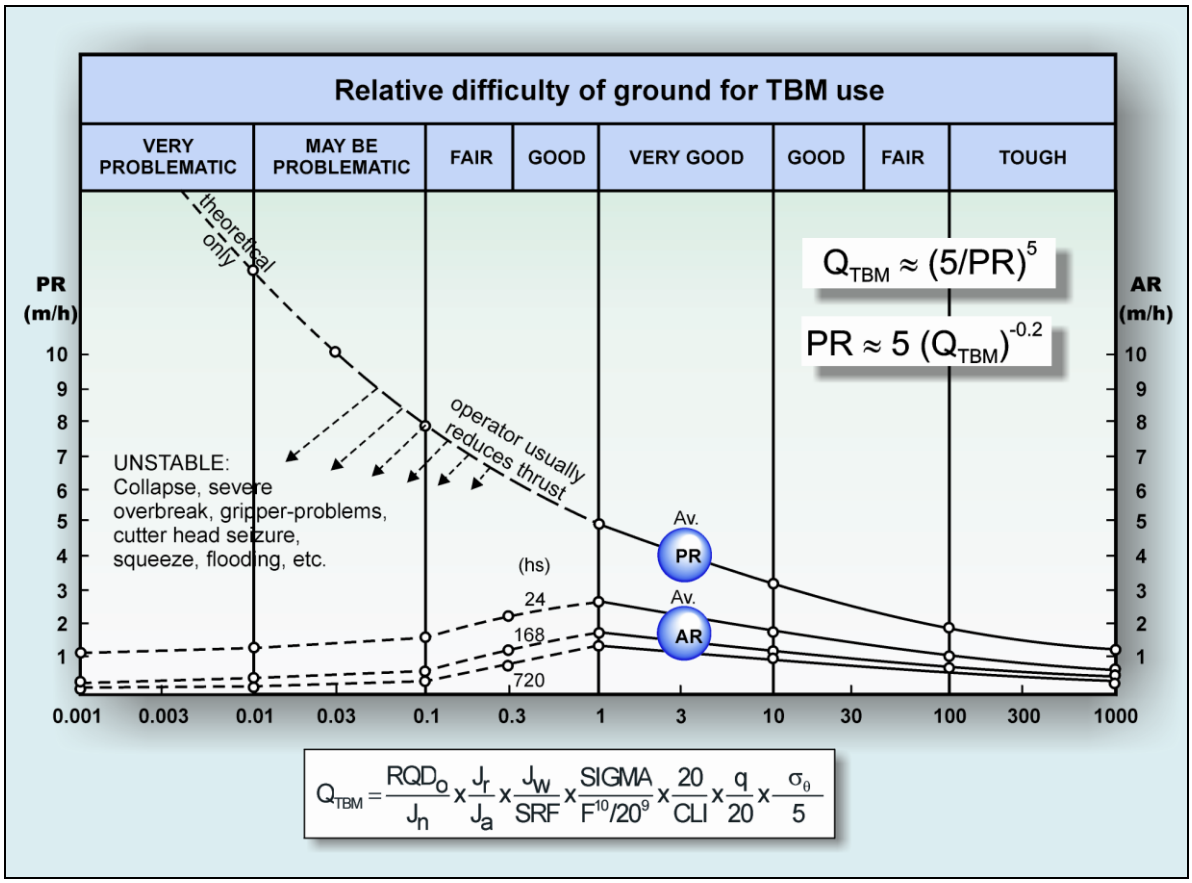

Figure 53. The theoretical (and empirical) basis for the Q_{TBM} calculations, using the program 'Qtbm'. Barton and Abrahao, 2003.

Why do fault zones take so long with TBM?

Practical reasons are illustrated in Figures 3, 10 and 54 (below, from Robbins, 1982). Theoretical (or ***theo-empirical***) reasons are given in the following simple equations, from Barton, 2000.

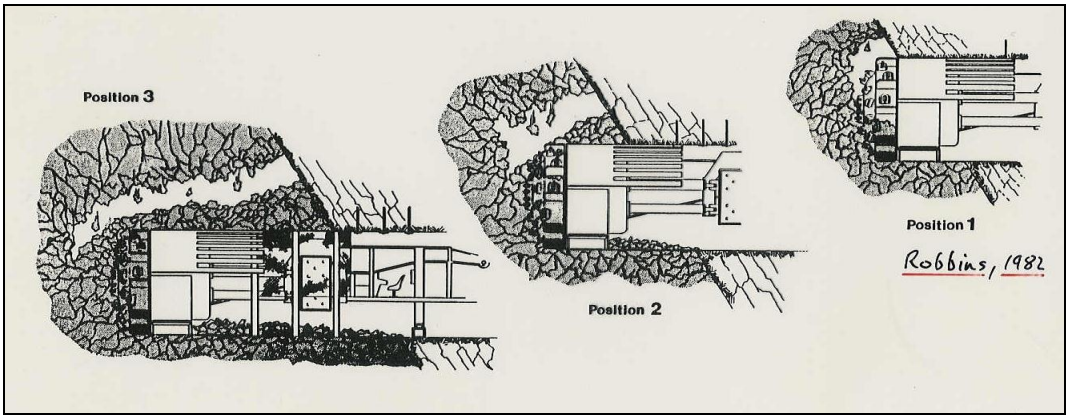

*Figure 54. Without probe drilling it is easy to be optimistic, especially when making world record speeds on other sections of the project. Robbins, 1982. Probe drilling is not usually done **under** the invert where first warnings would be detected, in this and many other cases.*

There are unfortunately very good 'theo-empirical' reasons why fault zones are so difficult for TBM (with or without double-shields).

We need three basic equations to start with

1. $AR = PR \times U$ (all TBM must follow this)
2. $U = T^m$ (due to the reducing **u**tilization with time, **a**dvance **r**ate decelerates)
3. $T = L / AR$ (obviously time needed for length L must be equal to L/AR)

Therefore we have the following

4. $T = L / (PR \times T^m)$ (from #1, #2 and #3)

5. $\underline{T = (L / PR)^{(1 / 1+m)}}$

6. This is very important equation for TBM, if one accepts that (-)***m*** is strongly related to Q-values in FAULT ZONES (as shown in the repeated figure below)

7. It is important because very ***negative*** **(-)m** values make (1/1+m) ***too big***

8. If the fault zone is wide (large L) and PR is low (due to collapses etc.) then L/PR gets too big to tolerate a big component (1/1+m) in equation 5.

9. It is easy (too easy) to calculate an almost 'infinite' time for a fault zone using this 'theo-empirical' equation. The writer knows of three permanently buried, or fault-destroyed TBM (Pont Ventoux, Dul Hasti, Pinglin). There are certainly many more, and the causes are probably related to equation 5 logic.

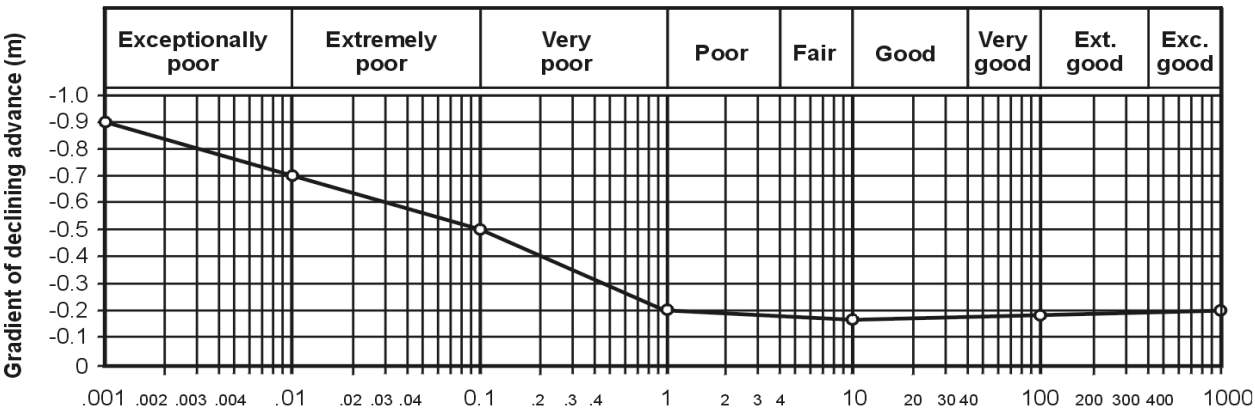

Rock mass quality $\mathbf{Q} = \left(\frac{\mathbf{RQD}}{\mathbf{J_n}}\right) \times \left(\frac{\mathbf{J_r}}{\mathbf{J_a}}\right) \times \left(\frac{\mathbf{J_w}}{\mathbf{SRF}}\right)$

Fault zones will remain a serious threat to TBM tunnelling as we now know it, unless the extremely poor rock mass qualities associated with fault zones ***can be improved by pre-grouting.***

Benefit of pre-injection is greatest when Q<1.0

In drill-and-blast tunnelling, thorough pre-injection around the complete (360º) profile can be more easily performed than when *'there is a TBM in the way'. T*he 20 to 24 hours (approx.) needed to drill and inject 20 to 40 holes of about 25m length is balanced by relatively trouble-free advance (of e.g. 4 or 5 rounds) through this (previously) bad ground, until the next cycle of pre-injection is performed to secure the next rounds. Typically 20 to 25m/week tunnel advance can be achieved on a regular basis, despite the (previously) bad ground.

Roald *(*in Barton et al. 2000/2001) has shown that time and cost of tunnelling are strongly correlated to Q-values when the Q-value is less than about 1.0, in fact just the same area of sensitivity to Q shown by TBM ***deceleration gradients (-m)*** (see figure on previous page). (The sensitivity to Q actually begins at about Q=10 where support increases begin).

So if the effective Q-value can be improved by pre-grouting – in the case of ***both drill-and-blast and TBM tunnelling,*** the greatest benefit will be achieved where the *Q-versus-cost* and *Q-versus-time curves* are steepest (about 0.01<Q<1.0).

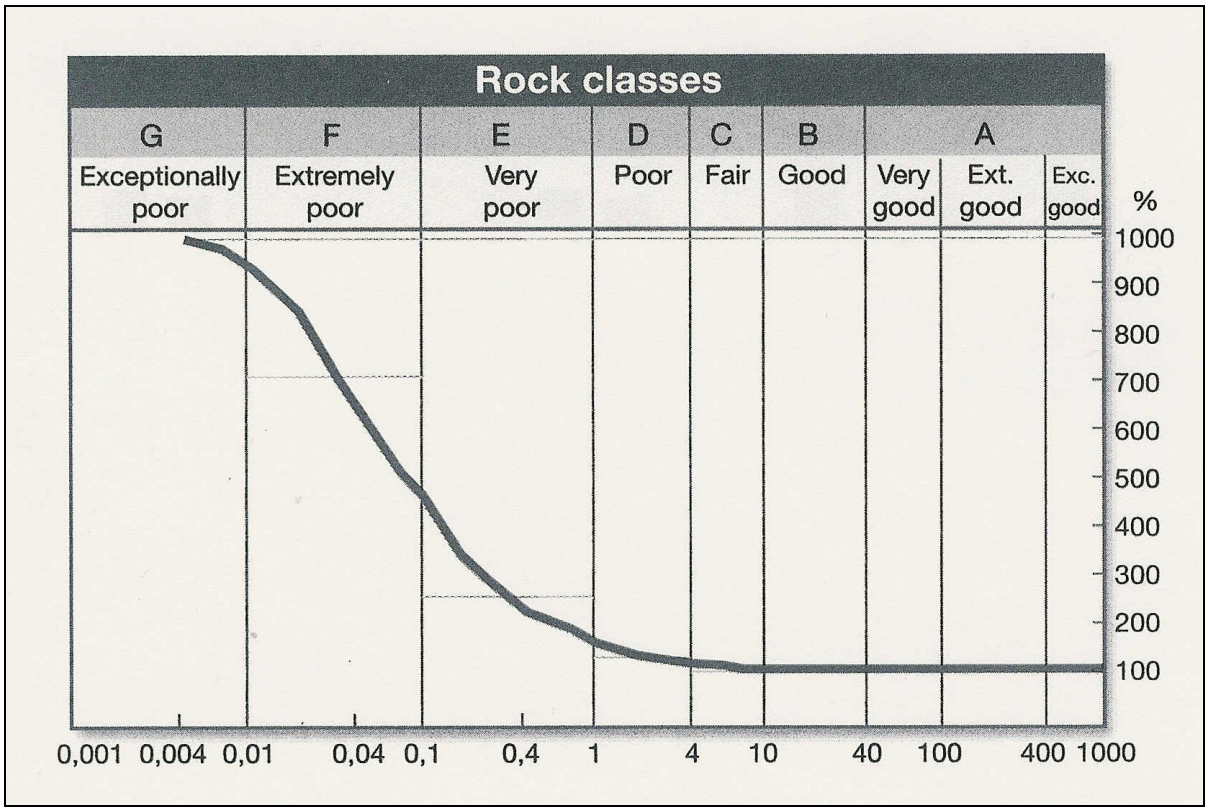

Figure 55. Relative time used in drill-and-blast tunnelling (support included), in relation to Q-value. Barton et al. 2000/2001. (Relative cost curve is similar, but the vertical axis extends to 1200%).

Are long tunnels faster by TBM?

It was shown in Figure 17 that 'central' rock qualities are required for TBM to be significantly faster than drill-and-blast. Figure 17 is repeated here as a reminder.

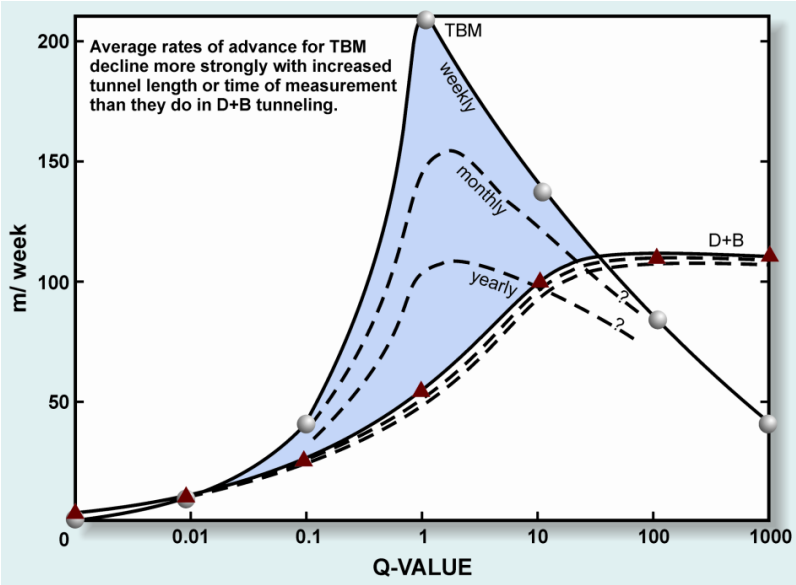

As tunnel length increases, this 'centrality' of rock quality becomes more important due to the deceleration of advance rate with time, and therefore with tunnel length.

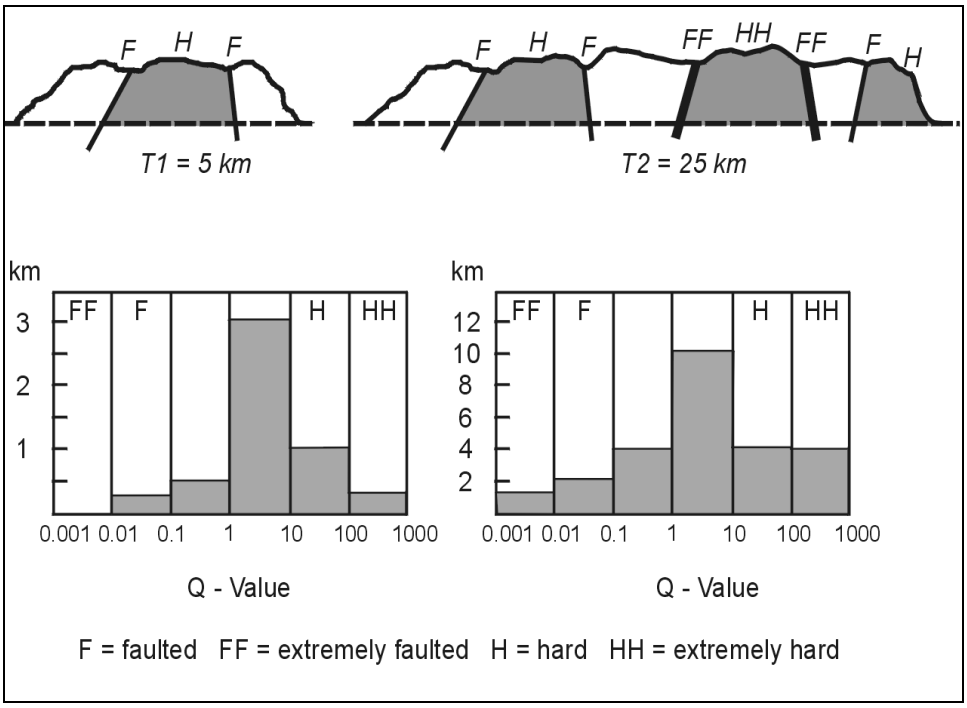

Figure 56. One should not blindly assume that long tunnels are faster by TBM. The longer the tunnel, the more likely that 'extreme value' statistics (of rock quality) will apply, due to a 'large scale' Weibull theory: i.e. more 'flaws' the larger the 'sample'. Barton, 2002.

Examples of a long tunnel that did not go faster by TBM

Pinglin Tunnel in NE Taiwan is an example of a TBM tunnel (actually three parallel tunnels) where serious faults caused such large cumulative delays, that drill-and-blast 'rescue' from the other end was essential for completion, after some 12 years of struggle to drive this 15km long twin-road tunnel.

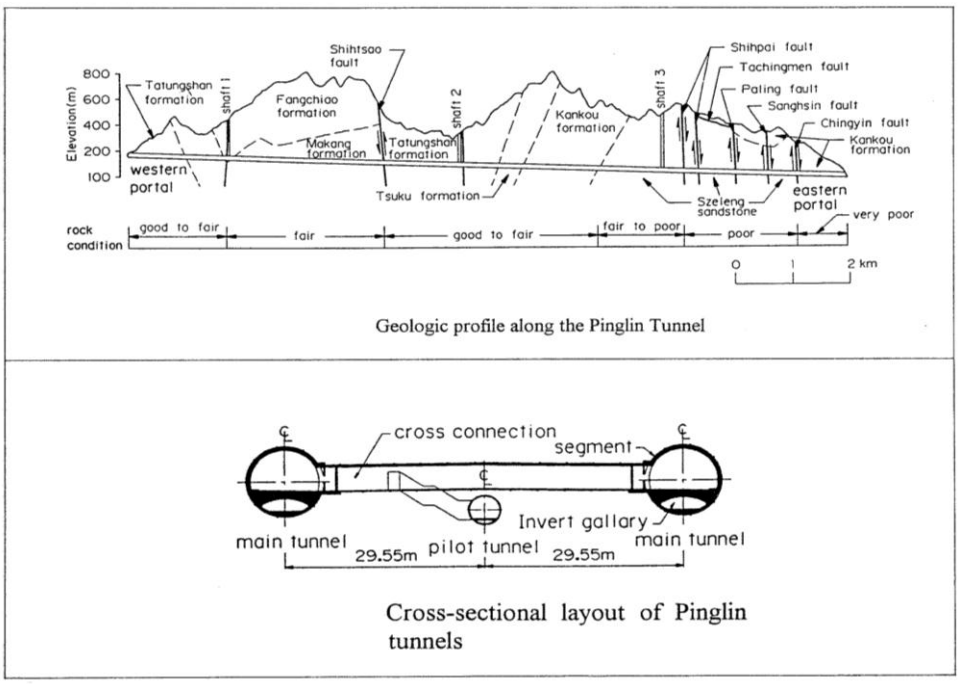

Figure 57. Geological section along Pinglin Tunnel, and cross-sectional layout of the three parallel tunnels.

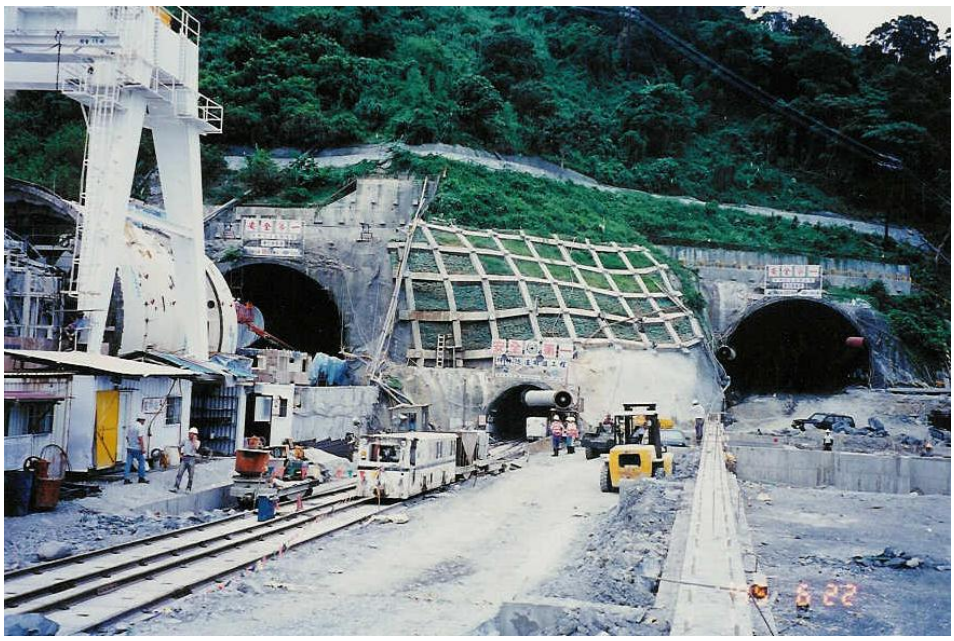

Figure 58. The Eastern portal in 1995, with the first running tunnel TBM under preparation, following advance excavation of part of the pilot TBM, which soon ran into stability problems.

Figure 59. The impressive Wirth TBM for Pinglin; two machines that eventually met rockmass conditions that frequently defeated them.

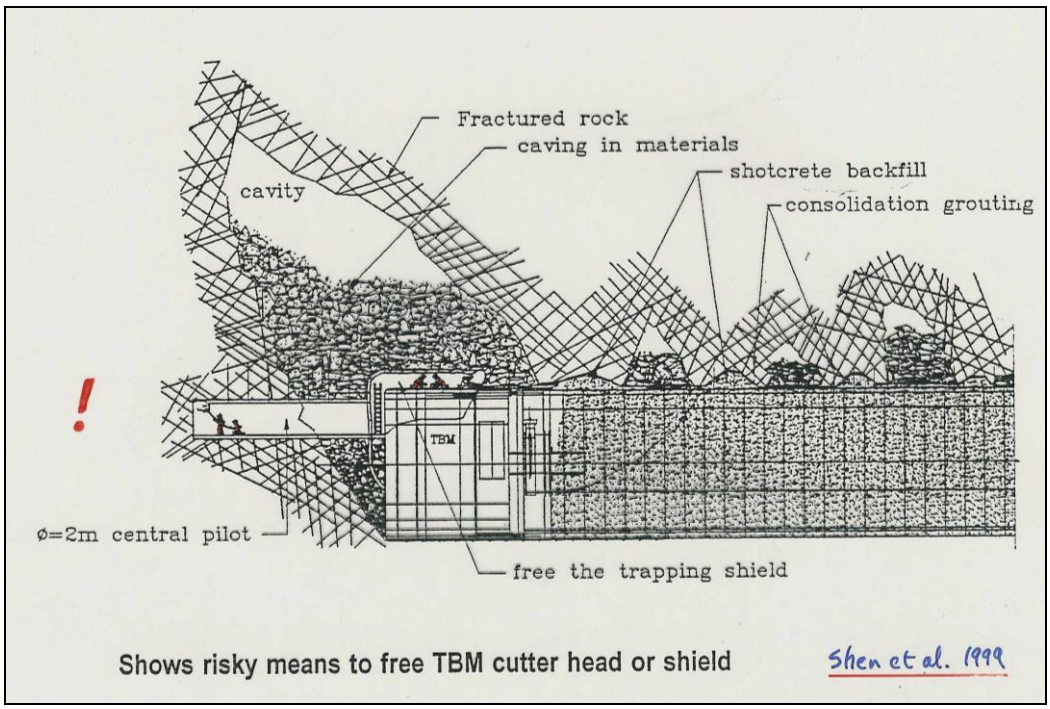

Figure 60. Graphic illustration of a by-pass situation for one of the Wirth TBM. The TBM was used to cut the bench material for significant lengths of problem ground, following the advance of a drill-and-blast top-heading. Shen et al. 1999.

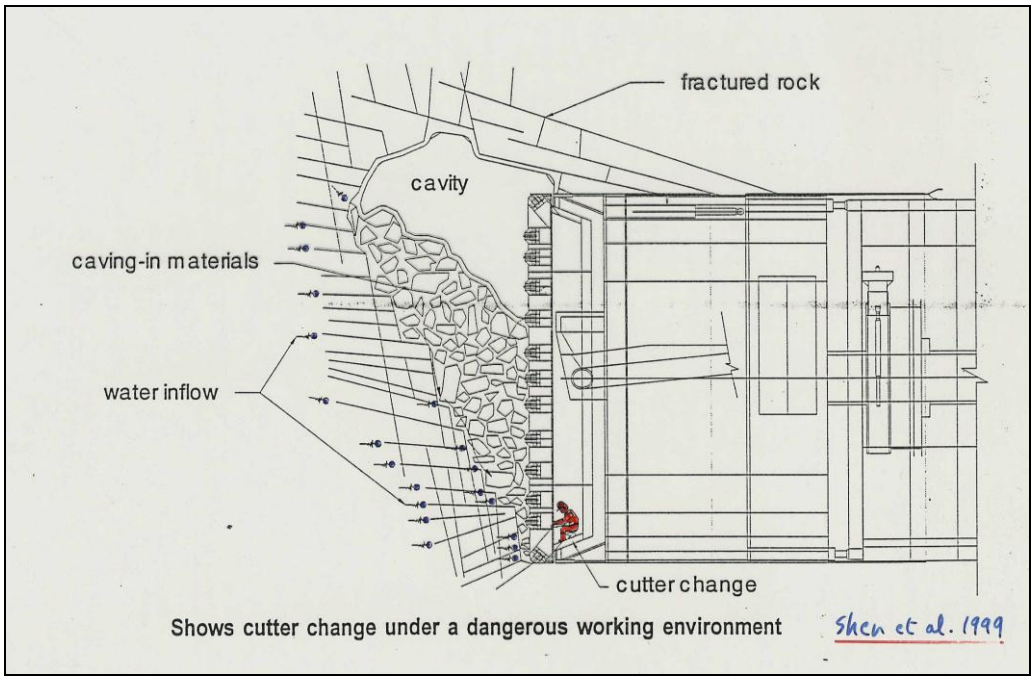

Figure 61. Difficult cutter change conditions in the meta-sandstones and quartzites of Pinglin. Shen et al. 1999.

Figure 62. A top-heading in advance of the stuck TBM. Note new breast-plating which was rapidly worn down by the abrasive conditions. C.Fong.

Figure 63. The 12th by-pass situation for the pilot TBM in 2002. C. Fong.

Figure 64. This is the running tunnel where earlier, one of the two 11.7m diameter TBM had been destroyed in a fault zone. At this 2002 location the actual face of this top-heading is 100m in front of the present 'face' due to a huge (and fatal) inrush of rock, clay and water. C. Fong.

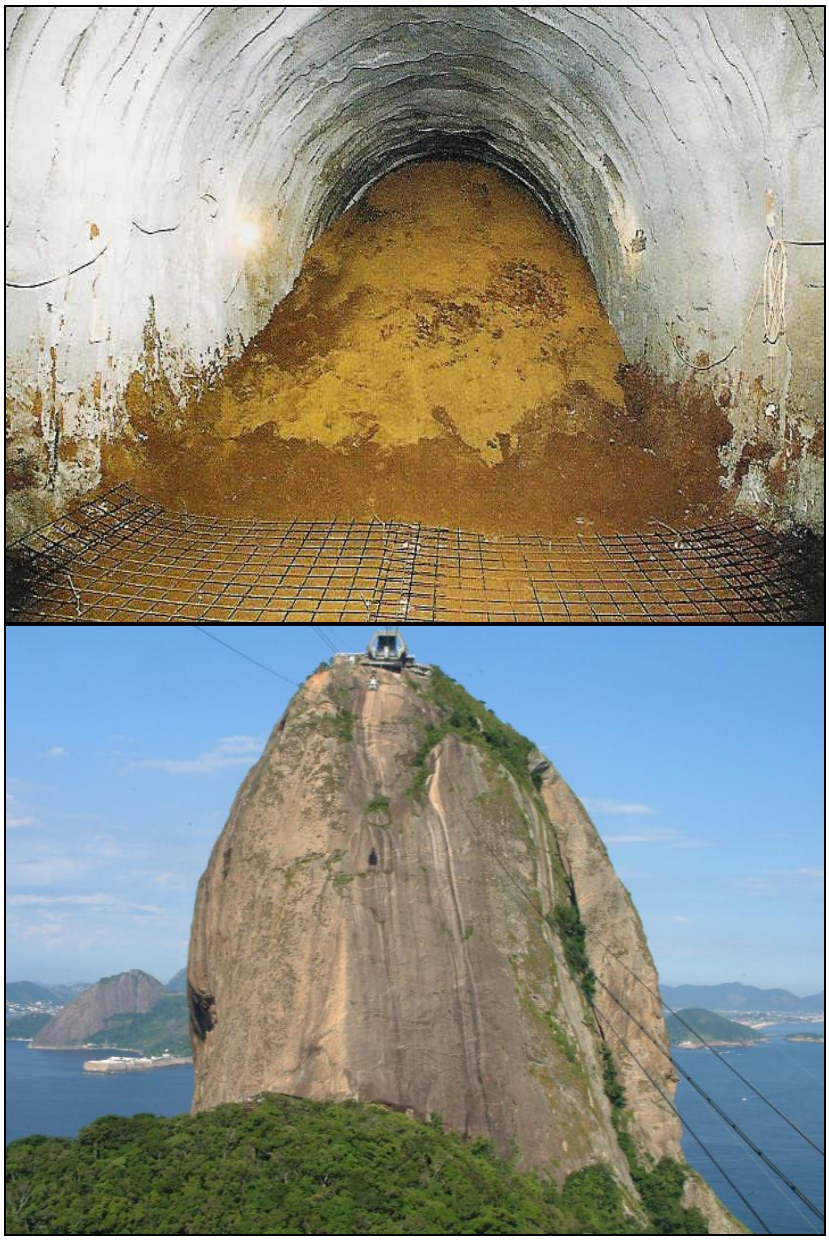

Figure 65. Two illustrations of (roughly-speaking) 'Q= 0.001' and 'Q=1000' 'rockmasses', that emphasise the advantage of a classification and characterization method that shows suitable numerical differentiation (1/1,000,000) of extreme qualities, when there is indeed a big difference in their properties (e.g. deformability, shear strength, 'compressive strength'). It is easier to develop simple equations that correlate Q with such properties, than is the case for classification systems that display only 1/10 or 1/20 numerical differentiation in such extremes, as for RMR and GSI.

Conclusions

1. Fault zones represent the ‘Achilles heel’ of TBM because, if sufficiently serious, they present the contractor with a situation where the TBM itself is actually ‘in the way’ of the most efficient pre-treatment or recovery methods that are usually available.

2. Fault zones are a form of ‘extreme value’ in terms of characterization or classification of the degree of difficulty (and support needs) that they represent. They therefore lie far outside the ideal ‘central’ qualities where TBM give advance rates that are much superior to those of drill-and-blast tunnelling.

3. Because TBM slowly decelerate as time and tunnel length increase, it is even more important that the rockmass has mostly ‘central’ qualities. So when a TBM is chosen ‘because the tunnel is very long and needs to be driven fast’, the opposite may actually occur, as extreme value statistics of rock quality are more likely to be encountered in a long tunnel, which possibly has high over-burden and reduced pre-investigation as a result.

4. Extreme values of rock quality, that may be ‘enhanced’ by the tunnel length being too long for the choice of TBM, include larger fault zones, higher water pressures, harder or more abrasive rock, and squeezing (or eroding) conditions in fault zones because of high over-burden (or high water pressures).

5. Double-shield machines, with PC-elements for both support and thrust (while re-setting grippers), have been claimed by some as the answer to ‘all’ variable rock conditions. Such a solution , at a significant extra cost, certainly produces a minimal deceleration gradient, in terms of minimising the slowing advance rate with increasing time or tunnel length, *when the rockmass conditions are not extreme.* When conditions are extreme, as when stuck in a significant fault zone, the time to recover and pre-treat the ground will tend to be longer, due to the now adverse total lengths of the (double) shields.

6. TBM tend to get stuck when several ‘predictable’ events combine into an unpredictable ‘unexpected events’ scenario, usually with extremely low Q-values. It is in avoidance of such situations that TBM can most benefit from probe drilling, *both downwards and upwards, and preferably to both sides as well.*

7. A degree of preparedness for approaching ‘no-longer-upredictable-unexpected-events’, can stimulate the use of drainage and systematic pre-injection, which is believed to effectively improve many (or all) of the six Q-parameters, thereby making advance less hazardous.

8. Beware of the effect of compaction or tunnel depth causing an increase in the seismic velocity, if using seismic profiling ahead of a (TBM) tunnel. The recording of a reasonable velocity of say 4km/s may mask actual fault zone qualities, which would reveal a 1.5 to 2Km/s velocity if encountered nearer the surface.

References

1. Barton, N., Lien, R. & Lunde, J. 1974. Engineering classification of rock masses for the design of tunnel support. Rock Mechanics. 6:4:189-236. Springer-Verlag.

2. Barton, N. 1995. The influence of joint properties in modelling jointed rock masses. Keynote Lecture, 8th ISRM Congress, Tokyo, 3: 1023-1032, Balkema, Rotterdam.

3. Barton, N. & Warren, C. 1996. Rock mass classification of chalk marl in the UK Channel Tunnels. Channel Tunnel Engineering Geology Symposium, Brighton, September 1995.

4. Barton, N. 1996. Rock mass characterization and seismic measurements to assist in the design and execution of TBM projects. Proc. of 1996 Taiwan Rock Engineering Symposium, Keynote Lecture, pp. 1-16.

5. Barton, N. 1999. TBM performance estimation in rock using Qtbm. Tunnels and Tunnelling International, Sept. 1999, pp. 30-34.

6. Barton, N. 2000. TBM tunnelling in jointed and faulted rock. 173p. Balkema, Rotterdam.

7. Barton, N. 2001. Are long tunnels faster by TBM? Proc. Rapid Excavation and Tunnelling Conf. RETC, San Diego, USA. Soc. Min. Eng., 819-828.

8. Barton, N., Buen, B. & Roald, S. 2001. Strengthening the case for grouting. Tunnels & Tunnelling International, Dec. 2001: 34-36, and Jan. 2002: 37-39.

9. Barton, N. 2002. Some new Q-value correlations to assist in site characterization and tunnel design. Int. J. Rock Mech. & Min. Sci. Vol. 39/2:185-216.

10. Barton, N. & de Quadros, E. 2003. Improved understanding of high pressure pre-grouting effects for tunnels in jointed rock. Proc. of 10th ISRM Congress, South Africa, Vol.1, 85-91.

11. Barton, N. 2003. TBM or drill and blast. Tunnels and Tunnelling International, 20-23, June.

12. Barton, N. and Abrahao, R. 2003. Employing the Q_{TBM} prognosis model. Tunnels and Tunnelling International, 20-23, December.

13. Bradley, W.B. 1978. Failure of inclined boreholes. Transactions of the American Society of Mechanical Engineers. 101:232-239.

14. Deva, Y., Dayal, H.M. & Mehrotra, A. 1994. Artesian blowout in a TBM driven water conductor tunnel in Northwest Himalaya, India. *Proc. 7th IAEG congress, Lisbon*. Oliveira et al. (eds) 4347-4354. Rotterdam: Balkema.

15. Grandori, R., Jaeger, M., Antonini, F. & Vigl, L. 1995. Evinos-Mornos Tunnel - Greece. Construction of a 30 km long hydraulic tunnel in less than three years under the most adverse geological conditions. *Proc. RETC. San Francisco, CA.* Williamson & Gowring (eds). 747-767. Littleton, CO: Soc. for Mining, Metallurgy, and Exploration, Inc.

16. Robbins, R.J. 1982. The application of tunnel boring machines to bad rock conditions. *ISRM symposium, Aachen.* 2: 827-836. Rotterdam: Balkema.

17. Shen, C.P., Tsai, H.C., Hsieh, Y.S. & Chu, B. 1999. The methodology through adverse geology ahead of Pinglin large TBM. *Proc. RETC. Orlando, FL*. Hilton & Samuelson (eds). Ch.8: 117-137.Littleton, CO: Soc. for Mining, Metallurgy, and Exploration, Inc.

18. Wanner, H. 1980. Stability problems by fullface tunnel boring. Fjellsprengningsteknikk. Bergmekanikk/Geoteknikk. 25.1-25.7. Trondheim: Tapir Press.